

1 SARS-CoV-2 spike protein induces the cytokine release syndrome by stimulating T cells to  
2 produce more IL-2

3 Chao Niu<sup>1,3</sup> <sup>†</sup>, Tingting Liang<sup>1, <sup>†</sup></sup>, Yongchong Chen<sup>1</sup>, Shan Zhu<sup>1, 2</sup>, Lei Zhou<sup>1</sup>, Naifei Chen<sup>1</sup>, Lei  
4 Qian<sup>1</sup>, Yufeng Wang<sup>1, 4</sup>, Min Li<sup>1, \*</sup>, Xin Zhou<sup>1, 3, 4, \*</sup>, Jiuwei Cui<sup>1, 4, \*</sup>

5

<sup>6</sup> <sup>1</sup> Cancer Center, The First Hospital of Jilin University, Changchun 130021, China

<sup>7</sup> <sup>2</sup> Institute of Translational Medicine, The First Hospital of Jilin University, Changchun 130021,  
<sup>8</sup> China

<sup>9</sup> <sup>3</sup> International Center of Future Science, Jilin University, Changchun 130021, China

<sup>4</sup> Cancer Research Institute of Jilin University, The First Hospital of Jilin University, Changchun 130021, China

12 <sup>†</sup> These authors share senior authorship.

13 Chao Niu E-mail: chaoniu@jlu.edu.cn

14 Tingting Liang E-mail: liangtt@jlu.edu.cn

15 Yongchong Chen E-mail: cycjdyy@jlu.edu.cn

16 Shan Zhu E-mail: zhus239@jlu.edu.cn

17 Lei Zhou E-mail: zhoulei@jlu.edu.cn

18 Naifei Chen E-mail: chennaifei@jlu.edu.cn

19 Lei Qian E-mail: qianlei\_cool@jlu.edu.cn

20 Yufeng Wang E-mail: Yufeng\_Wang@jlu.edu.cn

21 Min Li E-mail: limin1984@jlu.edu.cn

## 22 **Running title: IL-2 and spike protein promote cytokine release**

23

24 \* Correspondence:

25 Jiuwei Cui

26 [cuijw@jlu.edu.cn](mailto:cuijw@jlu.edu.cn)

27 Phone number: +86-43188782178

28 Fax number: +86-431-88786134

29

30 Xin Zhou

31 xinzhou@jlu.edu.cn

32 Phone number: +86-43188782046

33 Fax number: +86-431-88786134

34 **Abstract**

35 Cytokine release syndrome (CRS) is one of the leading causes of mortality in COVID-19 patients  
36 caused by the SARS-CoV-2 coronavirus. However, the mechanism of CRS induced by SARS-CoV-  
37 2 is vague. This study shows that dendritic cells loaded with spike protein of SARS-CoV-2 stimulate  
38 T cells to release much more IL-2, which subsequently cooperates with spike protein to facilitate  
39 peripheral blood mononuclear cells to release IL-1 $\beta$ , IL-6, and IL-8. These effects are achieved via  
40 IL-2 stimulation of NK cells to release TNF- $\alpha$  and IFN- $\gamma$ , as well as T cells to release IFN- $\gamma$ .  
41 Mechanistically, IFN- $\gamma$  and TNF- $\alpha$  enhance the transcription of CD40, and the interaction of CD40  
42 and its ligand stabilizes the membrane expression of TLR4 which serves as a receptor of spike  
43 protein on the surface of monocytes. As a result, there is a constant interaction between spike protein  
44 and TLR4, leading to continuous activation of NF- $\kappa$ B. Furthermore, TNF- $\alpha$  also activates NF- $\kappa$ B  
45 signaling in monocytes, which further cooperates with IFN- $\gamma$  and spike protein to modulate NF- $\kappa$ B-  
46 dependent transcription of CRS-related inflammatory cytokines. Targeting TNF- $\alpha$ /IFN- $\gamma$  in  
47 combination with TLR4 may represent a promising therapeutic approach for alleviating CRS in  
48 individuals with COVID-19.

49 **Keywords:** SARS-CoV-2, spike protein, monocyte, cytokine release syndrome, NF- $\kappa$ B, CD40

## 50 **Introduction**

51 COVID-19, caused by SARS-CoV-2, has become a global pandemic since its outbreak in 2019.(Hu  
52 et al., 2021) As of 12 April 2023, there have been 762,791,152 confirmed cases of COVID-19,  
53 including 6,897,025 deaths, reported to WHO. The clinical manifestations of severe COVID-19 are  
54 diverse, with acute respiratory distress syndrome, cytokine release syndrome (CRS), multiple organ  
55 failure, and death being the most notable.(Delorey et al., 2021; Wang & Perlman, 2022) CRS-related  
56 cytokines tend to increase progressively with the severity of the disease (Xiao et al., 2021) and may  
57 be the leading cause of life-threatening respiratory diseases in severe COVID-19 patients.(Que et  
58 al., 2022) Interestingly, it has been observed that the concentration of CRS-related cytokines is  
59 higher in the plasma of COVID-19 patients admitted to the intensive care unit (ICU) than in those  
60 who are not.(Huang et al., 2020) These cytokines include tumor necrosis factor (TNF)- $\alpha$ , interleukin  
61 (IL)-1 $\beta$ , IL-6, IL-10, IL-17, interferon (IFN)- $\gamma$  and IL-2, etc.(Giamarellos-Bourboulis et al., 2020;  
62 Mehta et al., 2020) However, the interplay between these cytokines remains unclear. Understanding  
63 the relationship between various cytokines in CRS is crucial for developing targeted therapies for  
64 COVID-19 and other cytokine storm syndromes.

65 Spike protein is one of the four main structural proteins of SARS-CoV-2, (Sen et al., 2021) which  
66 plays a crucial role in the virus's ability to enter the host cells as it can bind to the ACE2  
67 receptor.(Jackson et al., 2022) It also binds directly to pattern recognition receptor TLR4 to activate  
68 downstream signaling pathways which upregulate inflammatory factors such as IL-1 $\beta$  and IL-  
69 6.(Zhao et al., 2021a, 2021b) Therefore, spike protein may be a critical factor contributing to CRS  
70 in COVID-19 patients. The amount of spike protein increases with the increase of viral load.  
71 However, clinical studies have shown no significant difference in viral load between severe and  
72 mild COVID-19 patients, (To et al., 2020) and the viral load of patients with COVID-19 is relatively  
73 high in the initial stage of infection.(Pan et al., 2020; Walsh et al., 2020) These studies show that  
74 the accumulation of viral antigens may not be the leading cause of CRS. These findings indicate  
75 that factors other than the viral load may also significantly induce CRS in COVID-19 patients. The  
76 intricate interplay between spike protein, immune cells, and cytokines during the CRS remains  
77 largely unknown, highlighting the urgent need for further investigation.

78 During SARS-CoV-2 infection, alveolar macrophages play a critical role in detecting the virus and  
79 producing cytokines and chemokines to recruit innate and adaptive immune cells for virus  
80 elimination and disease prevention.(Gajjela & Zhou, 2022) Of note, macrophages and certain  
81 monocyte subsets are believed to be the decisive cells of CRS in patients with severe COVID-  
82 19.(Liao et al., 2020) Moreover, the over-activation of inflammatory response by other immune  
83 cells such as neutrophils, Dendritic cells (DCs), natural killer (NK) cells, B cells, and T cells can  
84 also contribute to CRS in this context.(Tan & Tang, 2021) Nonetheless, further research is still  
85 needed to determine the precise involvement of these cell types in CRS.

86 In this study, we investigated the mechanism underlying the development of CRS induced by SARS-  
87 Cov-2. Our finding suggests a cooperative effect of IL-2 and spike protein in stimulating peripheral  
88 blood mononuclear cells (PBMCs) to secrete IL-1 $\beta$ , IL-6, and IL-8. Mechanistically, DCs loaded  
89 with spike protein stimulate T cells to secrete IL-2, which subsequently facilitates the production of  
90 TNF- $\alpha$  and IFN- $\gamma$  by NK cells and IFN- $\gamma$  by T cells. Together, TNF- $\alpha$  and IFN- $\gamma$  make monocytes  
91 more active, and when stimulated by spike protein of SARS-CoV-2, these cells can release more  
92 CRS-related cytokines. Overall, our findings provide insights into the possible mechanism  
93 underlying CRS in COVID-19 patients and illustrate the complex interplay among various cytokines.  
94 These findings may pave the way for developing novel therapeutic targets for treating CRS, thereby  
95 offering promising avenues for clinical interventions in patients with COVID-19.

96 **Results**

97 **IL-2 cooperates with spike protein to stimulate PBMCs to secrete IL-1 $\beta$ , IL-6, and IL-8**

98 In order to analyze whether spike protein can stimulate PBMCs to secrete IL-6 or IL-1 $\beta$ , PBMCs  
99 were treated with different concentrations of spike protein, and a dose-dependent increase in the  
100 secretion of IL-6 and IL-1 $\beta$  was observed (Figure 1A). Hereafter, 10 nM spike protein was used for  
101 further experiments unless otherwise specified. The stimulatory effect of spike protein was further  
102 confirmed by increased secretion of IL-1 $\beta$ , IL-6, and IL-8 upon treatment with spike protein in  
103 PBMCs (Figure S1). However, no significant changes were observed in the expressions of other  
104 cytokines such as IL-2, IL-4, IL-5, IL-10, IL-12, IL-17, TNF- $\alpha$ , IFN- $\alpha$ , or IFN- $\gamma$  (Figure S1). These  
105 results suggest that spike protein alone cannot stimulate PBMCs to release various inflammatory  
106 factors. This phenomenon differs from the induction of diverse cytokine release in severe patients  
107 with COVID-19, indicating that other antigens of COVID-19 or other immune cells may be involved  
108 in the process of CRS in the human body.

109 Among various cytokines involved in the CRS of COVID-19 patients, IL-2 has drawn our particular  
110 attention. This is due to the noticeable elevation of IL-2 in the plasma of many severe COVID-19  
111 patients (Akbari et al., 2020; Huang et al., 2020; J. Liu et al., 2020) and high-dose IL-2  
112 administration causes capillary leak syndrome, (Boyman & Sprent, 2012; van Haelst Pisani et al.,  
113 1991) a severe clinical manifestations of CRS.(Case et al., 2020) Although the source of IL-2  
114 remains elusive, these studies hint at the crucial role of IL-2 in developing CRS in severe COVID-  
115 19 patients. Spike protein is a virus antigen which can be recognized by antigen-producing cells,  
116 such as DCs. We examined the effect of DCs loaded with spike protein on T-cell activation and  
117 found that DCs loaded with spike protein can stimulate T cells to secrete higher levels of IL-2 than  
118 did control DCs (Figure 1B). Along this line, we observed an increased secretion of IL-1 $\beta$ , IL-6, IL-  
119 8, IL-4, IL-5, and IL-12 from PBMCs treated with the combination of IL-2 and spike protein, as  
120 compared with spike protein or IL-2 alone (Figure 1C). In contrast, IL-2 alone stimulated PBMCs  
121 to secrete IFN- $\gamma$ , TNF- $\alpha$ , IFN- $\alpha$ , IL-17, and IL-10, while the combination of spike protein and IL-2  
122 did not show any synergistic effect on the secretion of these cytokines (Figure 1D). Together, these

123 data suggest that IL-2 released by T cells activated by DCs stimulated with spike protein may serve  
124 as an amplifier in inducing CRS in COVID-19 patients in a manner of cooperation with spike protein.

125 **Monocytes are the critical cells for the cooperation between IL-2 and spike protein in**  
126 **stimulating PBMCs to secrete inflammatory cytokines**

127 IL-6 is a critical cytokine involved in the pathogenesis of CRS in COVID-19 patients. In severe  
128 cases of COVID-19, elevated levels of IL-6 have been observed and are believed to contribute to  
129 the systemic inflammatory response and organ damage seen in some patients.(B. Liu et al., 2020;  
130 Smoke et al., 2021) Therefore, as a readout, IL-6 was used to analyze which cells in PBMCs are  
131 responders or effectors of the synergistic effect of IL-2 and spike protein to release cytokines.  
132 Intracellular staining and flow cytometry analysis revealed that spike protein, rather than IL-2,  
133 significantly increased the production of IL-6 in monocytes in PBMCs, and the combination of spike  
134 protein and IL-2 further enhanced this effect (Figure 2A). However, no increase in the expression  
135 level of IL-6 was observed in NK cells, B cells, or T cells (Figure 2B). These findings indicate that  
136 IL-2 can stimulate monocytes in PBMCs to produce more IL-6 in cooperation with spike protein.  
137 To further determine the involvement of monocytes, they were removed from PBMCs and then  
138 stimulated with spike protein, IL-2, or spike protein combined with IL-2. Compared with in that  
139 PBMCs, the levels of various cytokines, including IL-1 $\beta$ , IL-6, IL-8, IL-4, IL-5, IL-12, IL-2, TNF-  
140  $\alpha$ , and IL-17 decreased significantly in the supernatant of PBMCs without monocytes after treatment  
141 with spike protein combined with IL-2. Of note, IL-1 $\beta$ , IL-6, and IL-8 levels also decreased  
142 significantly in the supernatant of PBMCs treated with spike protein after monocytes removal  
143 (Figure 2C). These results indicate that monocytes play an essential role in the cytokine secretion  
144 by PBMCs stimulated by spike protein or IL-2 in cooperation with spike protein.

145 **IL-2 activates NF- $\kappa$ B of monocytes via stimulating PBMCs to release TNF- $\alpha$  and IFN- $\gamma$**

146 To investigate the mechanism underlying the synergistic effect of IL-2 and spike protein in inducing  
147 CRS, transcriptomic analysis was conducted on PBMCs treated with PBS, spike protein, IL-2, or a  
148 combination of spike protein and IL-2. Our analysis revealed that stimulation with spike protein  
149 activated multiple signaling pathways, including NF- $\kappa$ B, TNF, and JAK-STAT in PBMCs (Figure  
150 S2A-C). Notably, the combination of IL-2 and spike protein further amplified the activation of NF-  
151  $\kappa$ B, TNF, Toll-like receptor, and JAK-STAT signaling pathways compared to spike protein alone  
152 (Figure 3A-C). Flow cytometry analysis showed that spike protein facilitated the phosphorylation  
153 of p65, an indicator of activation of the NF- $\kappa$ B signaling pathway, in monocytes within PBMCs,  
154 and IL-2 combined with spike protein further enhanced this effect (Figure 3D and S2D).

155 Significantly, inhibiting the activation of NF- $\kappa$ B with IKK-16 not only significantly reduced the  
156 secretion of IL-6, IL-1 $\beta$ , and IL-8 by PBMCs stimulated by spike protein (Figure S2E, S2F) but also  
157 blocked the secretion of these cytokines by PBMCs stimulated by IL-2 in cooperation with spike  
158 protein (Figure 3E-G). As TNF and JAK-STAT signaling pathways were significantly enriched in

159 PBMCs treated with IL-2 combined with spike protein compared to spike protein alone (Figure 3A,  
160 3B), it appears that IL-2 may regulate these pathways in PBMCs. The JAK-STAT signaling pathway  
161 is tightly regulated by IFN and plays an important role in various biological processes.(Di Bona et  
162 al., 2006; Li et al., 2023; O'Connell et al., 2015) Interestingly, in the IL-2 combined with spike  
163 protein group, TNF- $\alpha$  and IFN- $\gamma$  levels were significantly increased compared to the spike protein  
164 group (Figure 3H). IL-2 alone elevated TNF- $\alpha$  and IFN- $\gamma$  levels in PBMCs, too (Figure 1D).  
165 Importantly, blocking TNF- $\alpha$  or/and IFN- $\gamma$  with antibodies during PBMCs stimulation with IL-2  
166 combined with spike protein inhibited the activation of the NF- $\kappa$ B signaling pathway (Figure 3I).

167 Based on these findings, it can be inferred that IL-2 plays a crucial role in activating the NF- $\kappa$ B  
168 signaling pathway in PBMCs by promoting the secretion of TNF- $\alpha$  and IFN- $\gamma$ . Previous studies  
169 have reported that spike protein also activates the NF- $\kappa$ B signaling pathway.(Forsyth et al., 2022)  
170 Therefore, the interplay between IL-2 and TNF- $\alpha$ /IFN- $\gamma$  might be crucial in mediating the  
171 synergistic effect of IL-2 and spike protein in inducing CRS in COVID-19 patients.

172 **TNF- $\alpha$  and IFN- $\gamma$  cooperate with spike protein to stimulate monocytes to secrete IL-1 $\beta$ , IL-6,  
173 and IL-8**

174 As a critical transcription factor, NF- $\kappa$ B is involved in producing of many inflammatory cytokines,  
175 such as IL-1 $\beta$  and IL-6.(Al-Griw et al., 2022) Since the activation of NF- $\kappa$ B in PBMCs induced by  
176 IL-2 relies on TNF- $\alpha$  and IFN- $\gamma$  (Figure 3I), we sought to explore whether the secretion of CRS-  
177 related cytokines by PBMCs stimulated with IL-2 and spike protein also depends on these cytokines.  
178 Our results demonstrated that the TNF- $\alpha$  blocking antibodies effectively suppressed the secretion  
179 of IL-1 $\beta$ , IL-6, and IL-8 in PBMCs stimulated by IL-2 and spike protein. Similarly, the IFN- $\gamma$   
180 blocking antibodies inhibited the secretion of IL-1 $\beta$  and IL-6 in PBMCs stimulated under the same  
181 condition. Interestingly, the combined blocking effect of TNF- $\alpha$  and IFN- $\gamma$  was not significantly  
182 different from that of single blocking antibodies for TNF- $\alpha$  (Figure 4A), suggesting that TNF- $\alpha$   
183 plays a more important role in mediating IL-2-induced cytokines secretion, especially IL-8.  
184 Moreover, TNF- $\alpha$  or IFN- $\gamma$ , when combined with spike protein, stimulated the secretion of CRS-  
185 related cytokines in PBMCs, with the effect of their combination being the most potent (Figure 4B).  
186 Finally, we observed that IKK-16, an NF- $\kappa$ B inhibitor, completely inhibited the secretion of IL-1 $\beta$ ,  
187 IL-6, and IL-8 by PBMCs stimulated with TNF- $\alpha$  or IFN- $\gamma$  that is cooperating with spike protein  
188 (Figure S3). Collectively, TNF- $\alpha$  and IFN- $\gamma$  are indispensable in activating NF- $\kappa$ B and inducing  
189 CRS-related cytokines in PBMCs via cooperating with spike protein.

190 As we demonstrated that monocytes are the critical cells for the cooperation between IL-2 and spike  
191 protein in stimulating PBMCs to secrete inflammatory cytokines (Figure 2), we further tested the  
192 synergistic effect of TNF- $\alpha$ /IFN- $\gamma$  and spike protein in purified monocytes. As expected, TNF- $\alpha$  or  
193 IFN- $\gamma$ , when combined with spike protein, stimulated monocytes to secrete IL-1 $\beta$ , IL-6, and IL-8,  
194 with the most potent effect observed when spike protein was combined with TNF- $\alpha$  and IFN- $\gamma$   
195 (Figure 4C). However, surprisingly, there was no synergism observed when IL-2 was combined

196 with spike protein in purified monocytes (Figure 4C). These observations suggest that other immune  
197 cells are involved in mediating the synergistic effect of IL-2 and spike protein in PBMCs. Therefore,  
198 to test this hypothesis, we treated PBMCs and monocytes from the same volunteer with IL-2 and  
199 spike protein, and then measured cytokine levels in the supernatant. The results showed that the  
200 expressions of IL-1 $\beta$ , IL-6, and IL-8 in the supernatant of the monocyte group were remarkably lower  
201 than those in the PBMCs group from the same volunteer (Figure 4D). Of note, the induction of TNF-  
202  $\alpha$  and IFN- $\gamma$  was also strikingly lower in monocytes than in the PBMCs under the same stimulatory  
203 conditions, raising the possibility that the less potent effect of IL-2 and spike protein in monocytes  
204 as compared to PBMCs is due to the lower induction of TNF- $\alpha$  and IFN- $\gamma$  (Figure 4C). Overall,  
205 these results indicate that IL-2 and spike protein work together to stimulate other immune cells to  
206 release TNF- $\alpha$  and IFN- $\gamma$ , thereby facilitating monocytes to secrete IL-1 $\beta$ , IL-6, and IL-8.

207 **NK cells and T cells play essential roles in the synergistic stimulation of CRS-related cytokines  
208 by IL-2 and spike protein via IFN- $\gamma$  and TNF- $\alpha$**

209 To identify the immune cells responsible for secreting TNF- $\alpha$  and IFN- $\gamma$  in PBMCs stimulated by  
210 IL-2, we conducted intracellular staining to analyze the secretion of these cytokines in NK cells, T  
211 cells, B cells, and monocytes within PBMCs. Our results indicated that compared with the PBS  
212 control group, IL-2 could increase the secretion of TNF- $\alpha$  in NK cells and IFN- $\gamma$  in NK cells and T  
213 cells. Compared with the spike protein group, IL-2 combined with spike protein can promote the  
214 secretion of TNF- $\alpha$  in NK cells and monocytes and IFN- $\gamma$  in NK cells and T cells (Figure 5A, B).  
215 To further investigate the role of NK cells and T cells in the secretion of inflammatory factors by  
216 PBMCs stimulated by IL-2 and spike protein, we cocultured monocytes with NK cells or T cells,  
217 respectively, and then stimulated them with IL-2 and spike protein. Our finding showed that  
218 combining IL-2 and spike protein significantly elevated IL-1 $\beta$ , IL-6, and IL-8 in monocytes  
219 cocultured with T cells and those cocultured with NK cells (Figure 5C, D). However, stimulating  
220 monocytes alone did not have the same effect (Figure 5C). These data further support the notion  
221 that IL-2, in collaboration with spike protein, stimulates PBMCs to secrete IL-1 $\beta$ , IL-6, and IL-8,  
222 and this is dependent on the presence of NK cells and T cells.

223 **IL-2 induce an increase in the expression of CD40 and in turn facilitates the surface  
224 localization of TLR4 in monocytes via TNF- $\alpha$  and IFN- $\gamma$**

225 As we have demonstrated that NF- $\kappa$ B plays a critical role in mediating the synergistic effect of spike  
226 protein with IL-2, TNF- $\alpha$ , or IFN- $\gamma$  (Figure 3E, F and S3), we sought to explore its upstream  
227 responder to spike protein and these cytokines. Through high-throughput sequencing technology,  
228 we discovered significant activation of the Toll-like receptor signaling pathway in PBMCs in the  
229 present IL-2 combined with spike protein when compared to spike protein alone (Figure 3A, 6A).  
230 It has been reported that TLR4 is a receptor of spike protein (Zhao et al., 2021a, 2021b). As IL-1 $\beta$   
231 and IL-6 are classic downstream of the TLR4-NF- $\kappa$ B signaling cascade, IL-2, TNF- $\alpha$ , and IFN- $\gamma$   
232 may exert their effects via this pathway as well. We found that spike protein reduces the membrane

233 surface expression of TLR4 in monocytes of PBMCs (Figure 6B) without affecting its transcription  
234 (Figure 6C). Spike protein binding to TLR4 leads to the internalization of TLR4, which is consistent  
235 with the effect of LPS on TLR4. Interestingly, IL-2 combined with spike protein was found to  
236 reverse the effect of spike protein on decreasing TLR4 membrane expression without affecting its  
237 transcription (Figure 6B, C).

238 In recent studies, several proteins that regulate the stabilization, internalization, intracellular  
239 trafficking, and recycling of TLR4 have been identified.(Aerbajinai et al., 2013; Cao et al., 2016;  
240 Ciesielska et al., 2021; Kim & Kim, 2014; Liu et al., 2023; Tatematsu et al., 2016) We noticed a  
241 significant upregulation of CD40, which has been reported to be able to up-regulate membrane  
242 expression of TLR4 binding LPS,(Frleta et al., 2003) by IL-2 combined with spike protein compared  
243 to spike protein alone in PBMCs (Figure 6A). qPCR analysis confirmed that IL-2 significantly  
244 increased the transcription of CD40 in purified monocytes (Figure 6D) and also elevated its surface  
245 expression of monocytes in PBMCs (Figure 6E). Importantly, blocking antibodies against CD40  
246 strongly reduced the expression of TLR4 on the membrane surface of monocyte of PBMCs  
247 stimulated with IL-2 and spike protein (Figure 6F). The secretion of TLR4 downstream  
248 inflammatory cytokines such as IL-6, IL-1 $\beta$ , and IL-8 was also significantly inhibited upon CD40  
249 blocking (Figure S4), underscoring the vital role of CD40 in mediating the TLR4-NF- $\kappa$ B signaling  
250 pathway in response to synergistic stimulation of spike protein and IL-2.

251 Although IL-2 increased the expression of CD40 on monocytes in PBMCs, purified monocytes  
252 directly stimulated with IL-2 did not exhibit any significant increase in the expression of CD40 at  
253 all (Figure 6G). This finding suggests the involvement of other immune cells in CD40 regulation.  
254 Based on the data in Figure 3-5, we hypothesized that TNF- $\alpha$  or IFN- $\gamma$  might play a role in CD40  
255 regulation. Along this line, we found that TNF- $\alpha$  or IFN- $\gamma$  stimulated PBMCs markedly upregulated  
256 the expression of CD40 on the surface of monocytes in PBMCs, with IFN- $\gamma$  having a potency similar  
257 to IL-2 (Figure 6H). Notably, the expression of CD40 in monocytes stimulated by TNF- $\alpha$  or IFN- $\gamma$   
258 significantly increased, whereas IL-2 had no effect (Figure 6I, J), suggesting that TNF- $\alpha$  and IFN- $\gamma$   
259 may mediate the role of IL-2 in upregulating the expression of CD40 in PBMCs, as they are  
260 upregulated by IL-2 (Figure 3H). Furthermore, blocking antibodies against TNF- $\alpha$  or IFN- $\gamma$   
261 effectively attenuated the upregulation of CD40 on the surface of monocyte within PBMCs treated  
262 with IL-2 (Fig 6K) and reversed the upregulation of TLR4 on the surface of monocytes in PBMCs  
263 treated with spike protein and IL-2 (Figure 6L). These results suggest that the regulation of  
264 membrane expression CD40 and TLR4 in response to synergistic stimulation of spike protein and  
265 IL-2 is mediated by TNF- $\alpha$  and IFN- $\gamma$ . Moreover, we found that IKK-16, an inhibitor of NF- $\kappa$ B,  
266 could inhibit the promotion of TNF- $\alpha$  and IFN- $\gamma$  on CD40 expression (Figure 6M).

267 Considering the vital role of the TLR4-NF- $\kappa$ B signaling pathway in mediating the synergistic  
268 stimulation of spike protein and IL-2 in inducing inflammatory cytokines, this pathway presents a  
269 promising target for preventing or reducing CRS in COVID-19 patients. Consistent with the effect

270 of IKK-16, we found that TAK242, a TLR4 inhibitor, significantly inhibited the release of IL-1 $\beta$ ,  
271 IL-6, and IL-8 in PBMCs co-treated with IL-2 and spike protein (Figure 6N). Notably, this  
272 inhibitory effect was further enhanced when combined with blocking antibodies against TNF- $\alpha$  or  
273 IFN- $\gamma$  (Figure 6N).

274 Our findings suggested that IL-2 stimulation of PBMCs leads to a significant secretion of IFN- $\gamma$  and  
275 TNF- $\alpha$ , resulting in the upregulation of CD40 on the surface of monocytes. The increased interaction  
276 of CD40-CD40L then maintains the stable membrane localization of TLR4 and prolongs its  
277 interaction with spike protein, subsequently hyper-activating NF- $\kappa$ B in monocytes. These findings  
278 shed light on the mechanism underlying the synergistic effect of spike protein and IL-2 in inducing  
279 inflammatory cytokine release. They may provide important insights for developing effective  
280 therapeutic strategies to prevent or reduce CRS in patients with COVID-19.

## 281 Discussion

282 CRS is a common complication observed in severe COVID-19 patients.(Yongzhi, 2021) IL-6 and  
283 IL-1 are considered to be essential cytokines in CRS. We observed that spike protein can stimulate  
284 PBMCs to produce IL-1 $\beta$  and IL-6 in a dose-dependent manner. We initially speculated that an  
285 increase in viral load could lead to elevated spike protein levels and trigger CRS. However, there  
286 was no significant difference in viral load between severe and mild COVID-19 patients (To et al.,  
287 2020). Moreover, Clinical reports have shown that the viral load of patients with COVID-19 is  
288 relatively high in the initial stage of infection.(Pan et al., 2020; Walsh et al., 2020) These findings  
289 indicate that factors other than the viral load may play a more significant role in inducing CRS in  
290 COVID-19 patients.

291 One prominent feature of CRS in severe COVID-19 patients is the apparent increase in levels of  
292 cytokines. Many severe COVID-19 patients exhibit a noticeable elevation of IL-2 in their  
293 plasma.(Akbari et al., 2020; Huang et al., 2020; J. Liu et al., 2020) It has been reported that high-  
294 dose IL-2 administration causes capillary leak syndrome,(Boyman & Sprent, 2012; van Haelst  
295 Pisani et al., 1991) and coincidentally capillary leak syndrome is a severe clinical manifestation of  
296 CRS (Case et al., 2020). These studies hint at the crucial role of IL-2 in CRS in severe COVID-19  
297 patients. Along this line, our study revealed that DCs stimulated by spike protein activate T cells to  
298 release more IL-2 than those stimulated with DCs alone. Therefore, we speculate that spike protein  
299 may promote DCs to activate T cells to release a large amount of IL-2, leading to capillary leak  
300 syndrome in severe COVID-19 patients. Moreover, capillary leak syndrome also occurs in some  
301 individuals who received the SARS-CoV-2 RNA vaccine which translates and expresses spike  
302 protein *in vivo*,(Matheny et al., 2021) further supporting our speculation. IL-2 plays a critical role  
303 in the immune system, and we found that IL-2 alone can stimulate PBMCs to produce multiple  
304 cytokines (IFN- $\alpha$ , IFN- $\beta$ , TNF- $\alpha$ ), which may lead to the persist inflammation. Additionally, IL-2  
305 and spike protein of SARS-CoV-2 synergistically stimulated PBMCs to produce a large amount of  
306 IL-1 $\beta$ , IL-6, and IL-8. These results further reveal that the continuous presence of virus antigens

307 and persistent inflammatory reactions are the primary causes of CRS, which is consistent with the  
308 clinical symptoms of severe COVID-19 cases. Clinically, severe COVID-19 patients exhibit a slight  
309 decrease in viral load but persistent inflammatory reactions.(Moss, 2022; Zheng et al., 2020) Thus,  
310 our findings indicate that IL-2 is essential in CRS in patients with severe COVID-19.

311 Severe COVID-19 patients with CRS often exhibit activation of NF- $\kappa$ B, as well as upregulation of  
312 TNF- $\alpha$  and IFN- $\gamma$ .(Hariharan et al., 2021; Huang et al., 2020; Kircheis et al., 2020) However, the  
313 underlying mechanism is vague. In this study, we found that IL-2 activated the NF- $\kappa$ B pathway of  
314 monocytes by stimulating PBMCs to release TNF- $\alpha$  and IFN- $\gamma$ . It has been reported that spike  
315 protein of SARS-CoV-2 activates monocytes through binding to TLR4 which is an important  
316 upstream regulator of NF- $\kappa$ B.(Brando et al., 2021; Conte, 2021; Manik & Singh, 2022; Zhao et al.,  
317 2021b) We confirmed that spike protein activated the NF- $\kappa$ B, but when combined with IL-2, the  
318 NF- $\kappa$ B pathway becomes even more strongly activated. NF- $\kappa$ B inhibitor not only represses the NF-  
319  $\kappa$ B activation induced by spike protein or IL-2 combined with spike protein, but also reduces the  
320 release of IL-1 $\beta$ , IL-6, and IL-8 from PBMCs stimulated by IL-2 combined with spike protein.  
321 These indicate that the NF- $\kappa$ B is vital in the interplay between IL-2 and spike protein in inducing  
322 CRS-related inflammatory factors in PBMCs. Targeting the NF- $\kappa$ B pathway could, therefore, prove  
323 helpful in preventing and treating CRS in patients with COVID-19. It has been reported that aspirin  
324 may reduce mortality in patients with COVID-19,(Martha et al., 2021) but the mechanism is unclear.  
325 Since aspirin can inhibit NF- $\kappa$ B activity, (Huo et al., 2018; Liao et al., 2015) we speculate that  
326 aspirin may reduce the risk of severe CRS in COVID-19 patients by inhibiting the activity of NF-  
327  $\kappa$ B. Overall, our study clarified the interplay between IL-2, TNF- $\alpha$ , IFN- $\gamma$ , and CRS in COVID-19  
328 patients and highlighted potential avenues for therapeutic intervention.

329 We found that spike protein of SARS-CoV-2 reduces the membrane expression of TLR4 on  
330 monocytes, which may be due to the internalization of TLR4 after binding to its ligand.(Kagan et  
331 al., 2008) The internalized TLR4 locates at the endosome and involves in TRIF-dependent signaling  
332 pathways, leading to a decreased and delayed activation of NF- $\kappa$ B compared to the TLR4-MyD88  
333 signaling axis.(Lin et al., 2021) In addition, the internalized TLR4 would eventually be degraded by  
334 lysosomes, further weakening the NF- $\kappa$ B signaling activated by membrane TLR4.(Gangloff, 2012)  
335 Of note, after adding IL-2, the decrease in TLR4 membrane expression caused by spike protein was  
336 reversed, and the TLR4-NF- $\kappa$ B pathway was further activated. This occurred because IL-2  
337 maintained the stable localization of TLR4 on the surface of monocytes treated with spike protein  
338 by up-regulating the expression of CD40. The interaction between CD40 and CD40L helped  
339 stabilize TLR4 on the surface of monocytes treated with spike protein, thus avoiding its rapid  
340 internalization and degradation. Our research is consistent with previous reports in which they  
341 believe that the binding of CD40 and CD40L can improve the stability of TLR4 on the surface of  
342 DCs.(Frleta et al., 2003) Although IL-2 could not directly stimulate the expression of CD40 on  
343 monocytes, it achieved this effect through IFN- $\gamma$  and TNF- $\alpha$ . It should be noted that the impact of  
344 TNF- $\alpha$  was weaker than that of IFN- $\gamma$ , consistent with literature reports.(Lee et al., 2007) These

345 results indicate that TNF- $\alpha$  and IFN- $\gamma$  are crucial in enhancing the TLR4-NF- $\kappa$ B pathway via  
346 transcriptional regulation of CD40. Our study further showed that TNF- $\alpha$  neutralizing antibody  
347 combined with a TLR4 inhibitor inhibits the synergistic stimulation of IL-2 and spike protein in  
348 monocytes releasing CRS-related inflammatory factors such as IL-1 $\beta$ , IL-6, and IL-8. Therefore,  
349 the combination of TLR4 inhibitor and TNF- $\alpha$  neutralizing antibody may represent a promising  
350 therapeutic strategy in treating CRS in patients of COVID-19 and other syndromes, such as CAR-  
351 T cell anti-tumor therapy, where CRS is a common side effect.

352 Several clinical studies have shown that monocytes are involved in the developing of CRS in severe  
353 COVID-19 patients,(Falck-Jones et al., 2022; Ma et al., 2022; Merad & Martin, 2020; Pence, 2020)  
354 but currently, no effective *in vitro* model exists for verification. We found that when monocytes  
355 were removed from PBMCs, the synergistic effect of IL-2 and spike protein in stimulating PBMCs  
356 to release CRS-related cytokines significantly decreased. This indicated that our model could  
357 effectively certify that monocytes are the critical cells for releasing CRS-related cytokines. However,  
358 direct stimulation of monocytes with IL-2 combined with spike protein did not enhance the release  
359 of inflammatory factors, suggesting that IL-2 is not the primary factor directly cooperating with  
360 spike protein to stimulate monocytes to release inflammatory factors. Our study also found that  
361 PBMCs stimulated with IL-2 exhibited increased secretion of TNF- $\alpha$  and IFN- $\gamma$  from NK cells and  
362 IFN- $\gamma$  from T cells. Co-culturing NK cells or T cells with monocytes in the medium containing IL-  
363 2 and spike protein significantly increased the release of inflammatory factors, including IL-1 $\beta$ , IL-  
364 6, and IL-8. These findings further suggest that NK cells, T cells, and monocytes play an essential  
365 role in CRS induced by SARS-CoV-2. Our research provides novel insights into the interplay  
366 between immune cells and cytokines produced by CRS, laying the foundation for a better  
367 understanding of this severe complication related to COVID-19.

## 368 Conclusion

369 Our research suggests that after SARS-CoV-2 enters the human body, spike protein can activate  
370 DCs, which in turn stimulate T cells producing a large amount of IL-2. IL-2 can stimulate NK cells  
371 to release TNF- $\alpha$  and IFN- $\gamma$  and T cells to release IFN- $\gamma$ . The increased level of IFN- $\gamma$  enhances the  
372 membrane-located TLR4 via up-regulating the transcription of its partner CD40 in monocytes,  
373 resulting in prolonged interaction between spike protein and TLR4 and subsequent activation of  
374 NF- $\kappa$ B. Simultaneously, the elevated level of TNF- $\alpha$  activates the NF- $\kappa$ B signaling pathway of  
375 monocytes. In such a condition, TNF- $\alpha$  and IFN- $\gamma$  cooperate to enhance the activation of NF- $\kappa$ B-  
376 dependent transcription of CRS-related inflammatory cytokines such as IL-1 $\beta$ , IL-6, and IL-8  
377 (Figure 7). Overall, our study shows that the development of CRS requires the involvement of  
378 multiple immune cells, and IL-2, TNF- $\alpha$ , and IFN- $\gamma$  may act as the primary factors in triggering  
379 CRS, providing promising avenues for clinical interventions for COVID-19 patients.

## 380 Materials and Methods

381 ***Isolation of PBMCs***

382 The Ethics Committee of the First Hospital of Jilin University approved this study (2020-521). The  
383 peripheral blood samples rich in white blood cells were initially obtained from the Changchun  
384 Central Blood Station. PBMCs were obtained by Ficoll density gradient centrifugation of  
385 lymphocyte separation solution Lymphoprep™ (Axis-Shield, Oslo, Norway). PBMCs were  
386 cultured in RPMI-1640 medium (Gibco, Grand Island, NY, USA) in a humidified atmosphere with  
387 5% CO<sub>2</sub> at 37°C.

388 ***Spike protein stimulates PBMCs***

389 PBMCs were adjusted to 1×10<sup>6</sup> cells/mL RPMI-1640 medium, and the PBMCs were inoculated into  
390 24-well plates (NEST Biotechnology Co., Ltd, Wuxi, China) at 400 µL per well. Then PBS, spike  
391 protein (ACROBiosystems, Beijing, China), IL-2 (100 IU/mL), IL-2 (100 IU/mL) combined with  
392 spike protein (10 µM), TNF-α (0.5 ng/mL), TNF-α (0.5 ng/mL) combined with spike protein (10  
393 µM), IFN-γ (1 ng/mL), or IFN-γ (1 ng/mL) combined with spike protein (10 µM) (above cytokines  
394 were all from T&L Biological Technology, Beijing, China) were added to PBMCs. After 16 hrs of  
395 incubation, the supernatant was collected for cytokine detection. In some experiments, blocking  
396 antibodies against CD40 (10 µg/mL) (Biolegend, San Diego, USA), TNF-α (10 µg/mL)  
397 (MedChemExpress, Monmouth Junction, USA), or IFN-γ (10 µg/mL) (eBioscience, San Diego,  
398 USA) were added to the cultures.

399 ***Isolation of NK cells, T cells, and monocytes***

400 T cells, NK cells, and monocytes were isolated from PBMCs by EasySep Human T Cell Isolation  
401 Kit (StemCell Technologies, Vancouver, Canada), MACSxpress Whole Blood NK Cell Isolation  
402 Kit (Miltenyi Biotec, Bergisch Gladbach, Germany), and EasySep Human Monocyte Isolation Kit  
403 (StemCell Technologies). In the coculture experiment, the density of monocytes was adjusted to  
404 2×10<sup>5</sup> cells/mL, and NK or T cells were mixed with monocytes of corresponding donors according  
405 to the ratio of NK or T cells to monocytes. Cells were inoculated in 24-well plates at 400 µL per  
406 well. Then PBS, spike protein, IL-2, or IL-2 combined with spike protein were added respectively  
407 and incubated for 16 hrs. The supernatant was collected, and the cytokines in the supernatant were  
408 detected.

409 ***DCs and T cell coculture***

410 DCs were adjusted to 1×10<sup>6</sup> cells/mL in CellGenix® GMP DC serum-free medium (CellGenix,  
411 Freiburg, Germany) with 100 ng/mL GM-CSF and 50 ng/mL IL-4 (both from T&L Biological  
412 Technology). Spike protein and TNF-α were added on the fifth day of culture, and DCs were  
413 collected on the seventh day. The density of T cells was adjusted to 1×10<sup>6</sup> cells /mL, and DC and T  
414 cells were cocultured at a ratio of 1:5 for two days. The supernatant was collected for the detection  
415 of IL-2.

416 ***Flow cytometry***

417 The cell density should be adjusted to  $1 \times 10^6$  cells/mL, and then 1  $\mu$ L BD GolgiPlug<sup>TM</sup> (BD  
418 Biosciences, San Jose, CA, USA) should be added to each milliliter of the cell suspension. Cells  
419 were cultured in an incubator at 37°C for 4 h and washed with PBS once. Following the instructions  
420 of BD Cytofix/Cytoperm<sup>TM</sup> Plus Fixation/Permeabilization Solution Kit (BD Biosciences), Cells  
421 were fixed, permeabilized, and stained with anti-human TNF- $\alpha$  (Biolegend), anti-human IFN- $\gamma$  (BD  
422 Biosciences), anti-human IL-6 (Biolegend), or isotype control antibodies for 30 min.

423 To detect CD40 and TLR4 on monocytes, cells were adjusted to  $1 \times 10^6$  cells/mL and stained with  
424 anti-human CD14, anti-human CD40, anti-human TLR4, or isotype control antibodies (the above  
425 antibodies were all from Biolegend) at room temperature for 15 min.

426 PBMC should be adjusted to a cell density of  $2.5 \times 10^6$  cells/mL. An equal volume of BD Cytofix<sup>TM</sup>  
427 Fixation Buffer (BD Biosciences) was added to the cell suspension and fixed at 37°C for 10 min.  
428 After fixation, the cells were collected and mixed with 200  $\mu$ L BD PhosFlow<sup>TM</sup> Perm Buffer III  
429 (BD Biosciences), then incubated on ice for 30 minutes. The cells were washed with PBS twice and  
430 incubated with anti-human NF- $\kappa$ B p65 (pS529) (BD Biosciences), anti-human CD14, or isotype  
431 control antibodies for 30 min at room temperature in the dark.

432 After washing with PBS once, the cells were analyzed using a FACSaria II flow cytometer (BD  
433 Biosciences). The data were analyzed by FlowJo software version 10 (Tree Star, Inc., Ashland, OR,  
434 USA).

435 ***Cytokine detection***

436 Cytokines in the supernatants were assayed by Cytometric Bead Array (CBA, BD Biosciences) or  
437 respective ELISA kit (Biolegend) according to the manufacturer's instructions.

438 ***Quantitative Real-time PCR***

439 PBS, spike protein, IL-2, or IL-2 combined with spike protein were used to stimulate PBMCs for  
440 16h. Then monocytes were isolated by a monocyte enrichment kit. RNA of monocytes was extracted  
441 by GeneJET RNA Purification Kit (Thermo Fisher Scientific, Waltham, MA, USA), and cDNA was  
442 obtained by Hifair 1st Strand cDNA Synthesis SuperMix for qPCR (Yeasen, Shanghai, China).  
443 Quantitative real-time PCR (qPCR) was performed using 2 $\times$ RealStar Green Fast Mixture (GenStar,  
444 Beijing, China) in a CFX384 Real-Time System C1000 Touch Thermal Cycler (Bio-Rad  
445 Laboratories, Hercules, CA, USA). The relative transcription levels of the genes of interest were  
446 normalized against the expression of GAPDH and calculated using the  $\Delta\Delta$ CT method. The  
447 sequences of primers used in this study are CD40, CCTGTTGCCATCCTCTGGTG (forward  
448 primer) and AGCAGTGGAGCCAGGAAGA (reverse primer); TLR4,  
449 AGACCTGTCCTGAACCCTAT (forward primer) and CGATGGACTTCTAAACCAGCCA  
450 (reverse primer); GAPDH, GTCTCCTCTGACTTCAACAGCG (forward primer) and

451 ACCACCCTGTTGCTGTAGCCAA (reverse primer).

452 ***High throughput sequencing***

453 PBMCs were stimulated with PBS, spike protein, IL-2, or IL-2 combined with spike protein for 16  
454 hrs and used for RNA extraction using TRIzol™ reagent (Thermo Fisher Scientific, MA, USA)  
455 according to the manufacturer's instructions. RNA sequencing and bioinformatic analysis were  
456 performed at Shanghai Majorbio Bio-Pharm Technology Co., Ltd. (Shanghai, China). RNA  
457 sequencing data has been uploaded to the GEO database. GEO accession numbers is GSE241843.

458 ***Statistical analyses***

459 Statistical analysis was performed by GraphPad Prim 8 (GraphPad Software). Paired Student's t-  
460 test was performed for the comparison of two paired groups. One-way ANOVA or two-way  
461 ANOVA was conducted to compare three or more groups. *P* value of less than 0.05 was considered  
462 statistically significant.

463 ***Acknowledgments***

464 This work was supported by the National Key Research and Development Program of China under  
465 Grant number 2020YFA0707704, the Innovative Program of National Natural Science Foundation  
466 of China under Grant number 82050003, National Natural Science Foundation of China under Grant  
467 numbers 82273186, 82002962, and 81874052, Project funded by China Postdoctoral Science  
468 Foundation under Grant number 2021M691208, Jilin Provincial Science and Technology  
469 Department under Grant numbers 20200602032ZP, 20210401076YY, 20210303002SF and  
470 YDZJ202202CXJD004, Jilin Provincial Education Department under Grant number  
471 JJKH20221060KJ, Jilin Province Labor Resources and Social Security Department under Grant  
472 number 2023RY03, Jilin Provincial Development and Reform Commission under Grant number  
473 2021C010, and Changchun Science and Technology Bureau under Grant number 21ZGY28.

474 ***Data Availability Statement***

475 All data generated or analyzed during this study are included in this published article.

476 ***Conflict of Interest***

477 The authors declare that the research was conducted in the absence of any commercial or financial  
478 relationships that could be construed as a potential conflict of interest.

479 ***Reference***

480 Aerbjainai, W., Lee, K., Chin, K., & Rodgers, G. P. (2013). Glia maturation factor-gamma negatively  
481 modulates TLR4 signaling by facilitating TLR4 endocytic trafficking in macrophages. *J  
482 Immunol.*, 190(12), 6093-6103. <https://doi.org/10.4049/jimmunol.1203048>

483 Akbari, H., Tabrizi, R., Lankarani, K. B., Aria, H., Vakili, S., Asadian, F., Noroozi, S., Keshavarz, P., &

484 Faramarz, S. (2020). The role of cytokine profile and lymphocyte subsets in the severity of  
485 coronavirus disease 2019 (COVID-19): A systematic review and meta-analysis. *Life Sci*,  
486 258, 118167. <https://doi.org/10.1016/j.lfs.2020.118167>

487 Al-Griw, M. A., Salter, M. G., & Wood, I. C. (2022). Blocking of NF- $\kappa$ B/p38 MAPK pathways mitigates  
488 oligodendrocyte pathology in a model of neonatal white matter injury. *Acta Neurobiol  
489 Exp (Wars)*, 82(1), 52-64. <https://doi.org/10.55782/ane-2022-005>

490 Boyman, O., & Sprent, J. (2012). The role of interleukin-2 during homeostasis and activation of the  
491 immune system. *Nat Rev Immunol*, 12(3), 180-190. <https://doi.org/10.1038/nri3156>

492 Branda, S. C. S., Ramos, J. O. X., Dompieri, L. T., Godoi, E., Figueiredo, J. L., Sarinho, E. S. C.,  
493 Chelvanambi, S., & Aikawa, M. (2021). Is Toll-like receptor 4 involved in the severity of  
494 COVID-19 pathology in patients with cardiometabolic comorbidities? *Cytokine Growth  
495 Factor Rev*, 58, 102-110. <https://doi.org/10.1016/j.cytoogr.2020.09.002>

496 Cao, D., Luo, J., Chen, D., Xu, H., Shi, H., Jing, X., & Zang, W. (2016). CD36 regulates  
497 lipopolysaccharide-induced signaling pathways and mediates the internalization of  
498 Escherichia coli in cooperation with TLR4 in goat mammary gland epithelial cells. *Sci Rep*,  
499 6, 23132. <https://doi.org/10.1038/srep23132>

500 Case, R., Ramanik, A., Martin, P., Simpson, P. J., Harden, C., & Ataya, A. (2020). Systemic Capillary  
501 Leak Syndrome Secondary to Coronavirus Disease 2019. *Chest*, 158(6), e267-e268.  
502 <https://doi.org/10.1016/j.chest.2020.06.049>

503 Ciesielska, A., Matyjek, M., & Kwiatkowska, K. (2021). TLR4 and CD14 trafficking and its influence  
504 on LPS-induced pro-inflammatory signaling. *Cell Mol Life Sci*, 78(4), 1233-1261.  
505 <https://doi.org/10.1007/s00018-020-03656-y>

506 Conte, C. (2021). Possible Link between SARS-CoV-2 Infection and Parkinson's Disease: The Role  
507 of Toll-Like Receptor 4. *Int J Mol Sci*, 22(13). <https://doi.org/10.3390/ijms22137135>

508 Delorey, T. M., Ziegler, C. G. K., Heimberg, G., Normand, R., Yang, Y., Segerstolpe, A., Abbondanza,  
509 D., Fleming, S. J., Subramanian, A., Montoro, D. T., Jagadeesh, K. A., Dey, K. K., Sen, P.,  
510 Slyper, M., Pita-Juarez, Y. H., Phillips, D., Biermann, J., Bloom-Ackermann, Z., Barkas, N.,  
511 Ganna, A., Gomez, J., Melms, J. C., Katsyv, I., Normandin, E., Naderi, P., Popov, Y. V., Raju,  
512 S. S., Niezen, S., Tsai, L. T., Siddle, K. J., Sud, M., Tran, V. M., Vellarikkal, S. K., Wang, Y.,  
513 Amir-Zilberstein, L., Atri, D. S., Beechem, J., Brook, O. R., Chen, J., Divakar, P., Dorceus, P.,  
514 Engreitz, J. M., Essene, A., Fitzgerald, D. M., Fropf, R., Gazal, S., Gould, J., Grzyb, J., Harvey,  
515 T., Hecht, J., Hether, T., Jane-Valbuena, J., Leney-Greene, M., Ma, H., McCabe, C.,  
516 McLoughlin, D. E., Miller, E. M., Muus, C., Niemi, M., Padera, R., Pan, L., Pant, D., Pe'er, C.,  
517 Pfiffner-Borges, J., Pinto, C. J., Plaisted, J., Reeves, J., Ross, M., Rudy, M., Rueckert, E. H.,  
518 Siciliano, M., Sturm, A., Todres, E., Waghray, A., Warren, S., Zhang, S., Zollinger, D. R.,  
519 Cosimi, L., Gupta, R. M., Hacohen, N., Hibshoosh, H., Hide, W., Price, A. L., Rajagopal, J.,  
520 Tata, P. R., Riedel, S., Szabo, G., Tickle, T. L., Ellinor, P. T., Hung, D., Sabeti, P. C., Novak, R.,  
521 Rogers, R., Ingber, D. E., Jiang, Z. G., Juric, D., Babadi, M., Farhi, S. L., Izar, B., Stone, J. R.,  
522 Vlachos, I. S., Solomon, I. H., Ashenberg, O., Porter, C. B. M., Li, B., Shalek, A. K., Villani, A.  
523 C., Rozenblatt-Rosen, O., & Regev, A. (2021). COVID-19 tissue atlases reveal SARS-CoV-  
524 2 pathology and cellular targets. *Nature*, 595(7865), 107-113.  
525 <https://doi.org/10.1038/s41586-021-03570-8>

526 Di Bona, D., Cippitelli, M., Fionda, C., Camma, C., Licata, A., Santoni, A., & Craxi, A. (2006). Oxidative  
527 stress inhibits IFN-alpha-induced antiviral gene expression by blocking the JAK-STAT

528 pathway. *J Hepatol*, 45(2), 271-279. <https://doi.org/10.1016/j.jhep.2006.01.037>

529 Falck-Jones, S., Osterberg, B., & Smed-Sorensen, A. (2022). Respiratory and systemic monocytes,  
530 dendritic cells, and myeloid-derived suppressor cells in COVID-19: Implications for  
531 disease severity. *J Intern Med*. <https://doi.org/10.1111/joim.13559>

532 Forsyth, C. B., Zhang, L., Bhushan, A., Swanson, B., Zhang, L., Mamede, J. I., Voigt, R. M., Shaikh, M.,  
533 Engen, P. A., & Keshavarzian, A. (2022). The SARS-CoV-2 S1 Spike Protein Promotes  
534 MAPK and NF- $\kappa$ B Activation in Human Lung Cells and Inflammatory Cytokine Production  
535 in Human Lung and Intestinal Epithelial Cells. *Microorganisms*, 10(10).  
536 <https://doi.org/10.3390/microorganisms10101996>

537 Frleta, D., Noelle, R. J., & Wade, W. F. (2003). CD40-mediated up-regulation of Toll-like receptor  
538 4-MD2 complex on the surface of murine dendritic cells. *J Leukoc Biol*, 74(6), 1064-1073.  
539 <https://doi.org/10.1189/jlb.0203062>

540 Gajjela, B. K., & Zhou, M. M. (2022). Calming the cytokine storm of COVID-19 through inhibition  
541 of JAK2/STAT3 signaling. *Drug Discov Today*, 27(2), 390-400.  
542 <https://doi.org/10.1016/j.drudis.2021.10.016>

543 Gangloff, M. (2012). Different dimerisation mode for TLR4 upon endosomal acidification? *Trends  
544 Biochem Sci*, 37(3), 92-98. <https://doi.org/10.1016/j.tibs.2011.11.003>

545 Giamarellos-Bourboulis, E. J., Netea, M. G., Rovina, N., Akinosoglou, K., Antoniadou, A., Antonakos,  
546 N., Damoraki, G., Gkavogianni, T., Adami, M. E., Katsaounou, P., Ntaganou, M.,  
547 Kyriakopoulou, M., Dimopoulos, G., Koutsodimitropoulos, I., Velissaris, D., Koufaryris, P.,  
548 Karageorgos, A., Katrini, K., Lekakis, V., Lupsie, M., Kotsaki, A., Renieris, G., Theodoulou, D.,  
549 Panou, V., Koukaki, E., Koulouris, N., Gogos, C., & Koutsoukou, A. (2020). Complex Immune  
550 Dysregulation in COVID-19 Patients with Severe Respiratory Failure. *Cell Host Microbe*,  
551 27(6), 992-1000 e1003. <https://doi.org/10.1016/j.chom.2020.04.009>

552 Hariharan, A., Hakeem, A. R., Radhakrishnan, S., Reddy, M. S., & Rela, M. (2021). The Role and  
553 Therapeutic Potential of NF- $\kappa$ B Pathway in Severe COVID-19 Patients.  
554 *Inflammopharmacology*, 29(1), 91-100. <https://doi.org/10.1007/s10787-020-00773-9>

555

556 Hu, B., Guo, H., Zhou, P., & Shi, Z. L. (2021). Characteristics of SARS-CoV-2 and COVID-19. *Nat  
557 Rev Microbiol*, 19(3), 141-154. <https://doi.org/10.1038/s41579-020-00459-7>

558 Huang, C., Wang, Y., Li, X., Ren, L., Zhao, J., Hu, Y., Zhang, L., Fan, G., Xu, J., Gu, X., Cheng, Z., Yu,  
559 T., Xia, J., Wei, Y., Wu, W., Xie, X., Yin, W., Li, H., Liu, M., Xiao, Y., Gao, H., Guo, L., Xie, J.,  
560 Wang, G., Jiang, R., Gao, Z., Jin, Q., Wang, J., & Cao, B. (2020). Clinical features of patients  
561 infected with 2019 novel coronavirus in Wuhan, China. *Lancet*, 395(10223), 497-506.  
562 [https://doi.org/10.1016/S0140-6736\(20\)30183-5](https://doi.org/10.1016/S0140-6736(20)30183-5)

563 Huo, X., Zhang, X., Yu, C., Cheng, E., Zhang, Q., Dunbar, K. B., Pham, T. H., Lynch, J. P., Wang, D.  
564 H., Bresalier, R. S., Spechler, S. J., & Souza, R. F. (2018). Aspirin prevents NF- $\kappa$ B  
565 activation and CDX2 expression stimulated by acid and bile salts in oesophageal  
566 squamous cells of patients with Barrett's oesophagus. *Gut*, 67(4), 606-615.  
567 <https://doi.org/10.1136/gutjnl-2016-313584>

568 Jackson, C. B., Farzan, M., Chen, B., & Choe, H. (2022). Mechanisms of SARS-CoV-2 entry into cells.  
569 *Nat Rev Mol Cell Biol*, 23(1), 3-20. <https://doi.org/10.1038/s41580-021-00418-x>

570 Kagan, J. C., Su, T., Horng, T., Chow, A., Akira, S., & Medzhitov, R. (2008). TRAM couples endocytosis  
571 of Toll-like receptor 4 to the induction of interferon-beta. *Nat Immunol*, 9(4), 361-368.

572 <https://doi.org/10.1038/ni1569>

573 Kim, D., & Kim, J. Y. (2014). Anti-CD14 antibody reduces LPS responsiveness via TLR4  
574 internalization in human monocytes. *Mol Immunol*, 57(2), 210-215.  
575 <https://doi.org/10.1016/j.molimm.2013.09.009>

576 Kircheis, R., Haasbach, E., Lueftnegger, D., Heyken, W. T., Ocker, M., & Planz, O. (2020). NF-  
577 kappaB Pathway as a Potential Target for Treatment of Critical Stage COVID-19 Patients.  
578 *Front Immunol*, 11, 598444. <https://doi.org/10.3389/fimmu.2020.598444>

579 Lee, S. J., Qin, H., & Benveniste, E. N. (2007). Simvastatin inhibits IFN-gamma-induced CD40 gene  
580 expression by suppressing STAT-1alpha. *J Leukoc Biol*, 82(2), 436-447.  
581 <https://doi.org/10.1189/jlb.1206739>

582 Li, Y., Cui, H., Li, S., Li, X., Guo, H., Nandakumar, K. S., & Li, Z. (2023). Kaempferol modulates IFN-  
583 gamma induced JAK-STAT signaling pathway and ameliorates imiquimod-induced  
584 psoriasis-like skin lesions. *Int Immunopharmacol*, 114, 109585.  
585 <https://doi.org/10.1016/j.intimp.2022.109585>

586 Liao, D., Zhong, L., Duan, T., Zhang, R. H., Wang, X., Wang, G., Hu, K., Lv, X., & Kang, T. (2015).  
587 Aspirin Suppresses the Growth and Metastasis of Osteosarcoma through the NF-kappaB  
588 Pathway. *Clin Cancer Res*, 21(23), 5349-5359. <https://doi.org/10.1158/1078-0432.CCR-15-0198>

589 Liao, M., Liu, Y., Yuan, J., Wen, Y., Xu, G., Zhao, J., Cheng, L., Li, J., Wang, X., Wang, F., Liu, L., Amit,  
590 I., Zhang, S., & Zhang, Z. (2020). Single-cell landscape of bronchoalveolar immune cells  
591 in patients with COVID-19. *Nat Med*, 26(6), 842-844. <https://doi.org/10.1038/s41591-020-0901-9>

592 Lin, C., Wang, H., Zhang, M., Mustafa, S., Wang, Y., Li, H., Yin, H., Hutchinson, M. R., & Wang, X.  
593 (2021). TLR4 biased small molecule modulators. *Pharmacol Ther*, 228, 107918.  
594 <https://doi.org/10.1016/j.pharmthera.2021.107918>

595 Liu, B., Li, M., Zhou, Z., Guan, X., & Xiang, Y. (2020). Can we use interleukin-6 (IL-6) blockade for  
596 coronavirus disease 2019 (COVID-19)-induced cytokine release syndrome (CRS)? *J  
597 Autoimmun*, 111, 102452. <https://doi.org/10.1016/j.jaut.2020.102452>

598 Liu, J., Li, S., Liu, J., Liang, B., Wang, X., Wang, H., Li, W., Tong, Q., Yi, J., Zhao, L., Xiong, L., Guo, C.,  
599 Tian, J., Luo, J., Yao, J., Pang, R., Shen, H., Peng, C., Liu, T., Zhang, Q., Wu, J., Xu, L., Lu, S.,  
600 Wang, B., Weng, Z., Han, C., Zhu, H., Zhou, R., Zhou, H., Chen, X., Ye, P., Zhu, B., Wang, L.,  
601 Zhou, W., He, S., He, Y., Jie, S., Wei, P., Zhang, J., Lu, Y., Wang, W., Zhang, L., Li, L., Zhou,  
602 F., Wang, J., Dittmer, U., Lu, M., Hu, Y., Yang, D., & Zheng, X. (2020). Longitudinal  
603 characteristics of lymphocyte responses and cytokine profiles in the peripheral blood of  
604 SARS-CoV-2 infected patients. *EBioMedicine*, 55, 102763.  
605 <https://doi.org/10.1016/j.ebiom.2020.102763>

606 Liu, Y., Zhang, M., Zhong, H., Xie, N., Wang, Y., Ding, S., & Su, X. (2023). LncRNA SNHG16 regulates  
607 RAS and NF-kappaB pathway-mediated NLRP3 inflammasome activation to aggravate  
608 diabetes nephropathy through stabilizing TLR4. *Acta Diabetol*, 60(4), 563-577.  
609 <https://doi.org/10.1007/s00592-022-02021-8>

610 Ma, Y., Qiu, F., Deng, C., Li, J., Huang, Y., Wu, Z., Zhou, Y., Zhang, Y., Xiong, Y., Yao, Y., Zhong, Y.,  
611 Qu, J., & Su, J. (2022). Integrating single-cell sequencing data with GWAS summary  
612 statistics reveals CD16+monocytes and memory CD8+T cells involved in severe COVID-  
613 19. *Genome Med*, 14(1), 16. <https://doi.org/10.1186/s13073-022-01021-1>

614

615

616 Manik, M., & Singh, R. K. (2022). Role of toll-like receptors in modulation of cytokine storm  
617 signaling in SARS-CoV-2-induced COVID-19. *J Med Virol*, 94(3), 869-877.  
618 <https://doi.org/10.1002/jmv.27405>

619 Martha, J. W., Pranata, R., Lim, M. A., Wibowo, A., & Akbar, M. R. (2021). Active prescription of low-  
620 dose aspirin during or prior to hospitalization and mortality in COVID-19: A systematic  
621 review and meta-analysis of adjusted effect estimates. *Int J Infect Dis*, 108, 6-12.  
622 <https://doi.org/10.1016/j.ijid.2021.05.016>

623 Matheny, M., Maleque, N., Channell, N., Eisch, A. R., Auld, S. C., Banerji, A., & Druey, K. M. (2021).  
624 Severe Exacerbations of Systemic Capillary Leak Syndrome After COVID-19 Vaccination:  
625 A Case Series. *Ann Intern Med*, 174(10), 1476-1478. <https://doi.org/10.7326/L21-0250>

626

627 Mehta, P., McAuley, D. F., Brown, M., Sanchez, E., Tattersall, R. S., Manson, J. J., & Hlh Across  
628 Speciality Collaboration, U. K. (2020). COVID-19: consider cytokine storm syndromes and  
629 immunosuppression. *Lancet*, 395(10229), 1033-1034. [https://doi.org/10.1016/S0140-6736\(20\)30628-0](https://doi.org/10.1016/S0140-6736(20)30628-0)

631 Merad, M., & Martin, J. C. (2020). Pathological inflammation in patients with COVID-19: a key role  
632 for monocytes and macrophages. *Nat Rev Immunol*, 20(6), 355-362.  
633 <https://doi.org/10.1038/s41577-020-0331-4>

634 Moss, P. (2022). The T cell immune response against SARS-CoV-2. *Nat Immunol*, 23(2), 186-193.  
635 <https://doi.org/10.1038/s41590-021-01122-w>

636 O'Connell, D., Bouazza, B., Kokalari, B., Amrani, Y., Khatib, A., Ganther, J. D., & Tliba, O. (2015). IFN-  
637 gamma-induced JAK/STAT, but not NF-kappaB, signaling pathway is insensitive to  
638 glucocorticoid in airway epithelial cells. *Am J Physiol Lung Cell Mol Physiol*, 309(4), L348-  
639 359. <https://doi.org/10.1152/ajplung.00099.2015>

640 Pan, Y., Zhang, D., Yang, P., Poon, L. L. M., & Wang, Q. (2020). Viral load of SARS-CoV-2 in clinical  
641 samples. *Lancet Infect Dis*, 20(4), 411-412. [https://doi.org/10.1016/S1473-3099\(20\)30113-4](https://doi.org/10.1016/S1473-3099(20)30113-4)

643 Pence, B. D. (2020). Severe COVID-19 and aging: are monocytes the key? *Geroscience*, 42(4),  
644 1051-1061. <https://doi.org/10.1007/s11357-020-00213-0>

645 Que, Y., Hu, C., Wan, K., Hu, P., Wang, R., Luo, J., Li, T., Ping, R., Hu, Q., Sun, Y., Wu, X., Tu, L., Du,  
646 Y., Chang, C., & Xu, G. (2022). Cytokine release syndrome in COVID-19: a major  
647 mechanism of morbidity and mortality. *Int Rev Immunol*, 41(2), 217-230.  
648 <https://doi.org/10.1080/08830185.2021.1884248>

649 Sen, S., Dey, A., Bandhyopadhyay, S., Uversky, V. N., & Maulik, U. (2021). Understanding structural  
650 malleability of the SARS-CoV-2 proteins and relation to the comorbidities. *Brief Bioinform*,  
651 22(6). <https://doi.org/10.1093/bib/bbab232>

652 Smoke, S. M., Raja, K., Hilden, P., & Daniel, N. M. (2021). Early clinical outcomes with tocilizumab  
653 for severe COVID-19: a two-centre retrospective study. *Int J Antimicrob Agents*, 57(2),  
654 106265. <https://doi.org/10.1016/j.ijantimicag.2020.106265>

655 Tan, Y., & Tang, F. (2021). SARS-CoV-2-mediated immune system activation and potential  
656 application in immunotherapy. *Med Res Rev*, 41(2), 1167-1194.  
657 <https://doi.org/10.1002/med.21756>

658 Tatematsu, M., Yoshida, R., Morioka, Y., Ishii, N., Funami, K., Watanabe, A., Saeki, K., Seya, T., &  
659 Matsumoto, M. (2016). Raftlin Controls Lipopolysaccharide-Induced TLR4 Internalization

660 and TICAM-1 Signaling in a Cell Type-Specific Manner. *J Immunol*, 196(9), 3865-3876.  
661 <https://doi.org/10.4049/jimmunol.1501734>

662 To, K. K., Tsang, O. T., Leung, W. S., Tam, A. R., Wu, T. C., Lung, D. C., Yip, C. C., Cai, J. P., Chan, J.  
663 M., Chik, T. S., Lau, D. P., Choi, C. Y., Chen, L. L., Chan, W. M., Chan, K. H., Ip, J. D., Ng, A.  
664 C., Poon, R. W., Luo, C. T., Cheng, V. C., Chan, J. F., Hung, I. F., Chen, Z., Chen, H., & Yuen,  
665 K. Y. (2020). Temporal profiles of viral load in posterior oropharyngeal saliva samples and  
666 serum antibody responses during infection by SARS-CoV-2: an observational cohort  
667 study. *Lancet Infect Dis*, 20(5), 565-574. [https://doi.org/10.1016/S1473-3099\(20\)30196-1](https://doi.org/10.1016/S1473-3099(20)30196-1)

668

669 van Haelst Pisani, C., Kovach, J. S., Kita, H., Leiferman, K. M., Gleich, G. J., Silver, J. E., Dennin, R., &  
670 Abrams, J. S. (1991). Administration of interleukin-2 (IL-2) results in increased plasma  
671 concentrations of IL-5 and eosinophilia in patients with cancer. *Blood*, 78(6), 1538-1544.  
672 <https://www.ncbi.nlm.nih.gov/pubmed/1884020>

673 Walsh, K. A., Jordan, K., Clyne, B., Rohde, D., Drummond, L., Byrne, P., Ahern, S., Carty, P. G., O'Brien,  
674 K. K., O'Murchu, E., O'Neill, M., Smith, S. M., Ryan, M., & Harrington, P. (2020). SARS-CoV-  
675 2 detection, viral load and infectivity over the course of an infection. *J Infect*, 81(3), 357-  
676 371. <https://doi.org/10.1016/j.jinf.2020.06.067>

677 Wang, Y., & Perlman, S. (2022). COVID-19: Inflammatory Profile. *Annu Rev Med*, 73, 65-80.  
678 <https://doi.org/10.1146/annurev-med-042220-012417>

679 Xiao, N., Nie, M., Pang, H., Wang, B., Hu, J., Meng, X., Li, K., Ran, X., Long, Q., Deng, H., Chen, N.,  
680 Li, S., Tang, N., Huang, A., & Hu, Z. (2021). Integrated cytokine and metabolite analysis  
681 reveals immunometabolic reprogramming in COVID-19 patients with therapeutic  
682 implications. *Nat Commun*, 12(1), 1618. <https://doi.org/10.1038/s41467-021-21907-9>

683

684 Yongzhi, X. (2021). COVID-19-associated cytokine storm syndrome and diagnostic principles: an  
685 old and new issue. *Emerg Microbes Infect*, 10(1), 266-276.  
686 <https://doi.org/10.1080/22221751.2021.1884503>

687 Zhao, Y., Kuang, M., Li, J., Zhu, L., Jia, Z., Guo, X., Hu, Y., Kong, J., Yin, H., Wang, X., & You, F. (2021a).  
688 Publisher Correction: SARS-CoV-2 spike protein interacts with and activates TLR4. *Cell Res*, 31(7), 825. <https://doi.org/10.1038/s41422-021-00501-0>

689

690 Zhao, Y., Kuang, M., Li, J., Zhu, L., Jia, Z., Guo, X., Hu, Y., Kong, J., Yin, H., Wang, X., & You, F. (2021b).  
691 SARS-CoV-2 spike protein interacts with and activates TLR41. *Cell Res*, 31(7), 818-820.  
692 <https://doi.org/10.1038/s41422-021-00495-9>

693 Zheng, S., Fan, J., Yu, F., Feng, B., Lou, B., Zou, Q., Xie, G., Lin, S., Wang, R., Yang, X., Chen, W.,  
694 Wang, Q., Zhang, D., Liu, Y., Gong, R., Ma, Z., Lu, S., Xiao, Y., Gu, Y., Zhang, J., Yao, H., Xu,  
695 K., Lu, X., Wei, G., Zhou, J., Fang, Q., Cai, H., Qiu, Y., Sheng, J., Chen, Y., & Liang, T. (2020).  
696 Viral load dynamics and disease severity in patients infected with SARS-CoV-2 in Zhejiang  
697 province, China, January-March 2020: retrospective cohort study. *BMJ*, 369, m1443.  
698 <https://doi.org/10.1136/bmj.m1443>

699

700 **Figure Legends**

701 **Figure 1 IL-2 cooperates with spike protein to stimulate PBMCs to secrete IL-6, IL-1 $\beta$ , and**  
702 **IL-8.**

703 (A) Quantifying concentrations of IL-1 $\beta$  and IL-6 in supernatants of PBMCs stimulated by different  
704 concentrations of spike protein for 16 hrs according to CBA (n = 5 biological replicates). (B) Bar  
705 graph (right) showing the concentration of IL-2 in the supernatants of T cells cocultured with DC,  
706 DC activated with spike protein, spike protein, or PBS as indicated by the schema (left). n = 4  
707 biological replicates. (C, D) Quantifying concentrations of cytokines by CBA in the supernatants of  
708 PBMCs treated with PBS, spike protein, IL-2, or IL-2 combined with spike protein for 16 hrs (n =  
709 22 biological replicates). Data are presented as mean  $\pm$  SD. ns: not significant, \*p < 0.05, \*\*p <  
710 0.01, and \*\*\*p < 0.001 as analyzed by one-way ANOVA.

711

712 **Figure 2 Monocytes are pivotal cells in the secretion of CRS-related cytokines in PBMCs co-**  
713 **stimulated with IL-2 and spike protein.**

714 (A) Representative intracellular staining analysis (left) and quantification (right) of the expression  
715 of IL-6 by flow cytometry in monocytes of PBMCs stimulated with PBS, spike protein, IL-2, or  
716 spike protein combined with IL-2 for 16 hrs (n = 4 biological replicates). MFI, mean fluorescence  
717 intensity. (B) Quantification of the expression of IL-6 in NK cells, T cells, and B cells of PBMCs  
718 described in A. (C) Quantifying the concentrations of cytokines by CBA in the supernatants of  
719 PBMCs and PBMCs without monocytes stimulated with PBS, spike protein, IL-2, or spike protein  
720 combined with IL-2 for 16 hrs (n = 6 biological replicates). Data are presented as mean  $\pm$  SD. ns:  
721 not significant, \*p < 0.05, \*\*p < 0.01, and \*\*\*p < 0.001 as analyzed by one-way ANOVA (A, B)  
722 or two-way ANOVA (C).

723

724 **Figure 3 TNF- $\alpha$  and IFN- $\gamma$  mediate the activation of NF- $\kappa$ B in PBMCs upon the synergistic**  
725 **stimulation by spike protein and IL-2.**

726 (A) Bubble plot showing the enrichment of KEGG pathways based on the transcriptomic analysis  
727 of PBMCs treated with IL-2 combined with spike protein or spike protein alone for 16 hrs (n = 3  
728 biological replicates). (B) GSEA shows the TNF- $\alpha$  signaling via NF- $\kappa$ B and the IFN- $\gamma$  signatures in  
729 the transcriptomic analysis described in A. NES: normalized enrichment score; FDR: false  
730 discovery rate. (C) Heat map showing the differentially expressed genes in the NF- $\kappa$ B pathway in  
731 the samples in A. (D) Representative intracellular staining analysis (left) and quantification (right)  
732 of the expression of p-p65 by flow cytometry in monocytes of PBMCs stimulated with spike protein  
733 or spike protein combined with IL-2 for 16 hrs (n = 7 biological replicates). (E) Representative  
734 intracellular staining analysis (left) and quantification (right) of the expression of p-p65 in

735 monocytes of PBMCs stimulated with spike protein, spike protein combined with IL-2, or spike  
736 protein combined with IL-2 and IKK-16 for 16 hrs (n = 3 biological replicates). (F, G) Quantifying  
737 concentrations of IL-1 $\beta$ , IL-6, and IL-8 by CBA in the supernatants of PBMCs in E. (H) Quantifying  
738 concentrations of TNF- $\alpha$  and IFN- $\gamma$  in the supernatants of PBMCs stimulated with spike protein or  
739 spike protein combined with IL-2 for 16 hrs (n = 3 biological replicates). (I) Representative  
740 intracellular staining analysis (left) and quantification (right) of the expression of p-p65 in  
741 monocytes of PBMCs stimulated with spike protein, spike protein combined with IL-2 and control  
742 IgG, or spike protein combined with IL-2 and TNF- $\alpha$  or/and IFN- $\gamma$  blocking antibodies for 16 hrs  
743 (n = 3 biological replicates). Data are presented as mean  $\pm$  SD. ns: not significant, \*p < 0.05, \*\*p <  
744 0.01, and \*\*\*p < 0.001 as analyzed by paired Student's t-test (D and H) or one-way ANOVA (E, G,  
745 and I).

746

747 **Figure 4 TNF- $\alpha$  and IFN- $\gamma$  cooperate with spike protein to stimulate monocytes to release IL-  
748 1 $\beta$ , IL-6, and IL-8.**

749 (A) Quantifying concentrations of IL-1 $\beta$ , IL-6, and IL-8 by CBA in the supernatants of PBMCs  
750 stimulated with spike protein, spike protein combined with IL-2 together with/without blocking  
751 antibodies against TNF- $\alpha$  or IFN- $\gamma$  for 16 hrs (n = 4 biological replicates). (B) Quantifying  
752 concentrations of IL-1 $\beta$ , IL-6, and IL-8 by ELISA in the supernatants of PBMCs stimulated with  
753 spike protein, IL-2, TNF- $\alpha$ , IFN- $\gamma$ , or spike protein combined with these cytokines for 16 hrs (n = 8  
754 biological replicates). (C) Quantifying concentrations of IL-1 $\beta$ , IL-6, and IL-8 by CBA in the  
755 supernatants of monocytes stimulated with spike protein, IL-2, TNF- $\alpha$ , IFN- $\gamma$ , or spike protein  
756 combined with these cytokines for 16 hrs. (n = 7 biological replicates). (D) Quantifying  
757 concentrations of IL-1 $\beta$ , IL-6, IL-8, IFN- $\gamma$ , TNF- $\alpha$ , and IL-2 by CBA in the supernatants of PBMCs  
758 and monocytes stimulated with spike protein combined with IL-2 for 16 hrs. Each red line connects  
759 PBMCs and monocytes from the same donor. (n = 6 biological replicates) Data are presented as  
760 mean  $\pm$  SD. ns: not significant, \*p < 0.05, \*\*p < 0.01, and \*\*\*p < 0.001 as analyzed by one-way  
761 ANOVA (A, B, and C) or paired Student's t-test (D).

762

763 **Figure 5 T cells and NK cells play essential roles in the synergistic stimulation of CRS-related  
764 cytokines by IL-2 and spike protein via IFN- $\gamma$  and TNF- $\alpha$ .**

765 (A, B) Quantification of the expression of TNF- $\alpha$  and IFN- $\gamma$  by flow cytometry in NK cells,  
766 monocytes, T cells, and B cells of PBMCs stimulated with PBS, spike protein, IL-2, or spike protein  
767 combined with IL-2 for 16 hrs (n = 4 biological replicates). (C) Quantifying concentrations of IL-  
768 1 $\beta$ , IL-6, IL-8, IFN- $\gamma$ , and TNF- $\alpha$  by CBA in the supernatants of monocytes with/without  
769 cocultivation of T cells from the respective donor under stimulation with PBS, spike protein, IL-2,  
770 or spike protein combined with IL-2 for 16 hrs (n = 4 biological replicates). (D) Quantifying

771 concentrations of IL-1 $\beta$ , IL-6, IL-8, IFN- $\gamma$ , and TNF- $\alpha$  by CBA in the supernatants of monocytes  
772 cocultured with NK cells from the respective donor under stimulation with PBS, spike protein, IL-  
773 2, or spike protein combined with IL-2 for 16 hrs (n = 3 biological replicates). Data are presented  
774 as mean  $\pm$  SD. ns: not significant, \*p < 0.05, \*\*p < 0.01, and \*\*\*p < 0.001 as analyzed by one-way  
775 ANOVA.

776

777 **Figure 6 IL-2 induces an increase in the expression of CD40 and in turn facilitates the surface**  
778 **localization of TLR4 in monocytes via TNF- $\alpha$  and IFN- $\gamma$ .**

779 (A) GSEA and heat map showing the differentially expressed genes of TLR signaling pathway  
780 based on transcriptomic analysis in PBMCs treated with spike protein combined with IL-2 and spike  
781 protein alone for 16 hrs (n = 3 biological replicates). (B) Quantification of the expression of TLR4  
782 by flow cytometry on monocytes in PBMCs treated with PBS, spike protein, IL-2, or IL-2 combined  
783 with spike protein for 16 hrs (n = 7 biological replicates). (C, D) Quantification of the expression of  
784 TLR4 and CD40 by qPCR analysis in purified monocytes treated with PBS, spike protein, IL-2, or  
785 IL-2 combined with spike protein for 16 hrs (n = 3 biological replicates). (E) Representative staining  
786 analysis (left) and quantification (right) of the expression of CD40 by flow cytometry on monocytes  
787 in PBMCs stimulated with PBS, spike protein, IL-2, or spike protein combined with IL-2 for 16 hrs  
788 (n = 3 biological replicates). (F) Representative staining analysis (left) and quantification (right) of  
789 the expression of TLR4 on monocytes of PBMCs stimulated with spike protein combined with IL-  
790 2, along with the addition of CD40 blocking antibody or control IgG (n = 3 biological replicates).  
791 (G) Representative staining analysis of the expression of CD40 by flow cytometry on monocytes in  
792 PBMCs (left) and purified monocytes (right) treated with PBS or IL-2 for 16 hrs. (H) Representative  
793 staining analysis (left) and quantification (right) of the expression of CD40 by flow cytometry on  
794 monocytes in PBMCs stimulated by IL-2, TNF- $\alpha$ , or IFN- $\gamma$  for 16 hrs (n = 3 biological replicates).  
795 (I, J) Representative staining analysis (left) and quantification (right) of the expression of CD40 by  
796 flow cytometry on purified monocytes stimulated by IL-2, TNF- $\alpha$ , or IFN- $\gamma$  for 16 hrs (n = 3  
797 biological replicates). (K) Representative staining analysis (left) and quantification (right) of the  
798 expression of CD40 by flow cytometry on monocytes in PBMCs stimulated with IL-2 along with  
799 the addition of blocking antibodies against TNF- $\alpha$  or IFN- $\gamma$  or control IgG for 16 hrs (n = 5  
800 biological replicates). (L) Representative staining analysis (left) and quantification (right) of the  
801 expression of TLR4 by flow cytometry on monocytes in PBMCs stimulated with IL-2 combined  
802 with spike protein, along with the addition of blocking antibodies against TNF- $\alpha$  or IFN- $\gamma$  or control  
803 IgG for 16 hrs (n = 4 biological replicates). (M) Representative staining analysis (left) and  
804 quantification (right) of the expression of CD40 by flow cytometry on monocytes in PBMCs  
805 stimulated with TNF- $\alpha$  or IFN- $\gamma$  along with the addition of NF- $\kappa$ B inhibitor IKK-16 for 16 hrs (n =  
806 3 biological replicates). (N) Quantifying concentrations of IL-1 $\beta$ , IL-6, and IL-8 by CBA in the  
807 supernatants of PBMCs stimulated with spike protein combined with IL-2, along with the addition

808 of TLR4 inhibitor and blocking antibodies against TNF- $\alpha$  or IFN- $\gamma$  or control IgG for 16 hrs (n = 3  
809 biological replicates). Data are presented as mean  $\pm$  SD. ns: not significant, \*p < 0.05, \*\*p < 0.01,  
810 and \*\*\*p < 0.001 as analyzed by one-way ANOVA.

811

812 **Figure 7 A diagram of the mechanism of spike protein cooperating with IL-2 to stimulate**  
813 **immune cells to produce CRS-related inflammatory factors.**

814 DCs loaded with spike protein stimulate T cells to secrete IL-2, which subsequently facilitates the  
815 production of TNF- $\alpha$  and IFN- $\gamma$  by NK cells and IFN- $\gamma$  by T cells. IFN- $\gamma$  increases the transcription  
816 of CD40, which promotes the stable localization of TLR4 on the membrane surface of monocytes,  
817 leading to a constant interaction between spike protein and TLR4 and activation of NF- $\kappa$ B. TNF- $\alpha$   
818 also activates NF- $\kappa$ B signaling in monocytes, which cooperates with IFN- $\gamma$  to modulate NF- $\kappa$ B-  
819 dependent transcription of CRS-related inflammatory cytokines such as IL-1 $\beta$ , IL-6, and IL-8.

820

821 **Figure S1 Spike protein stimulates PBMCs to secrete IL-1 $\beta$ , IL-6, and IL-8.**

822 Quantifying concentrations of cytokines by CBA in the supernatants of PBMCs stimulated by spike  
823 protein for 16 hrs (n = 5 biological replicates). Data are presented as mean  $\pm$  SD. ns: not significant,  
824 \*p < 0.05, and \*\*p < 0.01 as analyzed by paired Student's t-test.

825

826 **Figure S2 Spike protein activates NF- $\kappa$ B to facilitate monocyte transcription of IL-1 $\beta$ , IL-6,**  
827 **and IL-8.**

828 (A) Bubble plot showing the enrichment of KEGG pathways based on the transcriptomic analysis  
829 of PBMCs treated with spike protein or PBS for 16 hrs. (B, C) Heat maps showing the differentially  
830 expressed genes in the NF- $\kappa$ B signaling pathway, TNF- $\alpha$  signaling pathway, and JAK-STAT  
831 signaling pathway in PBMCs treated with spike protein or PBS for 16 hrs (n = 3 biological  
832 replicates). (D) Representative intracellular staining analysis (left) and quantification (right) of the  
833 expression of p-p65 by flow cytometry in monocytes of PBMCs stimulated with spike protein or  
834 PBS for 16 hrs (n = 7 biological replicates). (E) Representative intracellular staining analysis (left)  
835 and quantification (right) of the expression of p-p65 by flow cytometry in monocytes of PBMCs  
836 stimulated with PBS, spike protein, or spike protein combined with IKK-16 (n = 3 biological  
837 replicates). (F) Quantifying concentrations of IL-1 $\beta$ , IL-6, and IL-8 by CBA in the supernatants of  
838 PBMCs stimulated with PBS, spike protein, or spike protein combined with IKK-16 for 16 hrs (n =  
839 3 biological replicates). Data are presented as mean  $\pm$  SD. ns: not significant, \*p < 0.05, \*\*p < 0.01,  
840 and \*\*\*p < 0.001 as analyzed by one-way ANOVA (E, F) or paired Student's t-test (D).

841

842 **Figure S3 Inhibition of NF-κB reduces the secretion of IL-1 $\beta$ , IL-6, and IL-8 in PBMCs**  
843 **stimulated by spike protein together with TNF- $\alpha$  or IFN- $\gamma$ .**

844 Quantifying concentrations of IL-1 $\beta$ , IL-6, and IL-8 by CBA in the supernatants of PBMCs  
845 stimulated with spike protein, spike protein combined with TNF- $\alpha$  or IFN- $\gamma$ , and spike protein  
846 combined with TNF- $\alpha$  or IFN- $\gamma$  together with IKK-16 for 16 hrs (n = 3 biological replicates). Data  
847 are presented as mean  $\pm$  SD. ns: not significant, \*p < 0.05, \*\*p < 0.01, and \*\*\*p < 0.001 as analyzed  
848 by one-way ANOVA.

849

850 **Figure S4 Reduction in the secretion of IL-1 $\beta$ , IL-6, and IL-8 in PBMCs stimulated with IL-2**  
851 **and spike protein upon blocking CD40.**

852 Quantifying concentrations of IL-1 $\beta$ , IL-6, and IL-8 by CBA in the supernatants of PBMCs  
853 stimulated with spike protein combined with IL-2 with/without CD40 blocking antibody for 16 hrs  
854 (n = 4 biological replicates). Data are presented as mean  $\pm$  SD. \*p < 0.05, and \*\*p < 0.01 as analyzed  
855 by paired Student's t-test.

856

Fig. 1

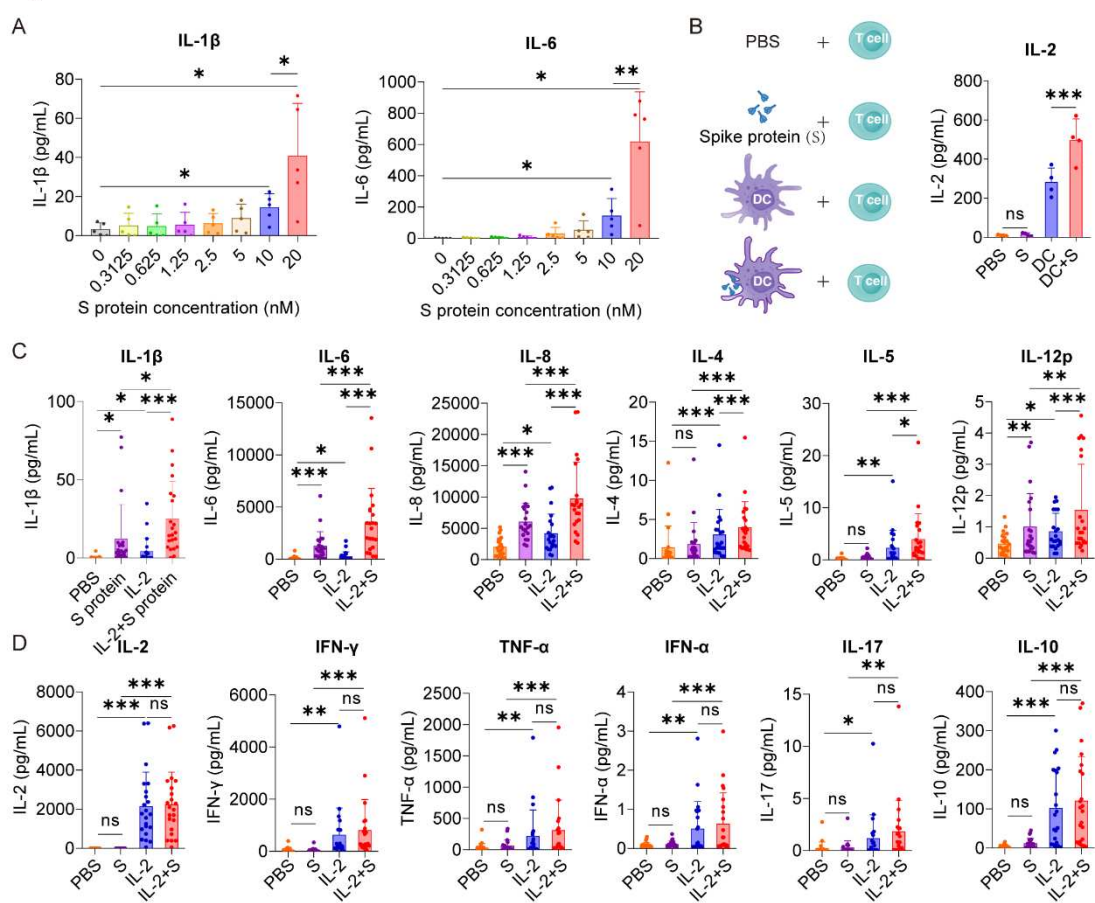
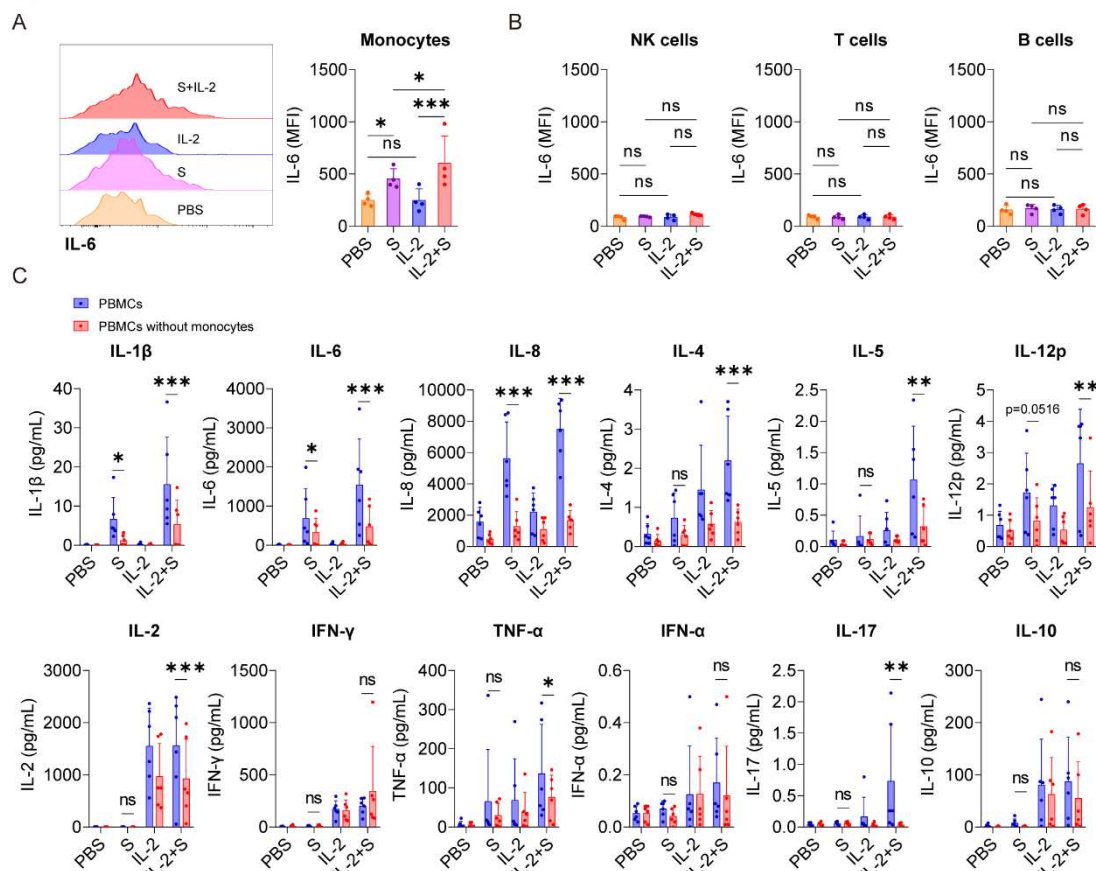


Fig. 2



858

859

Fig. 3

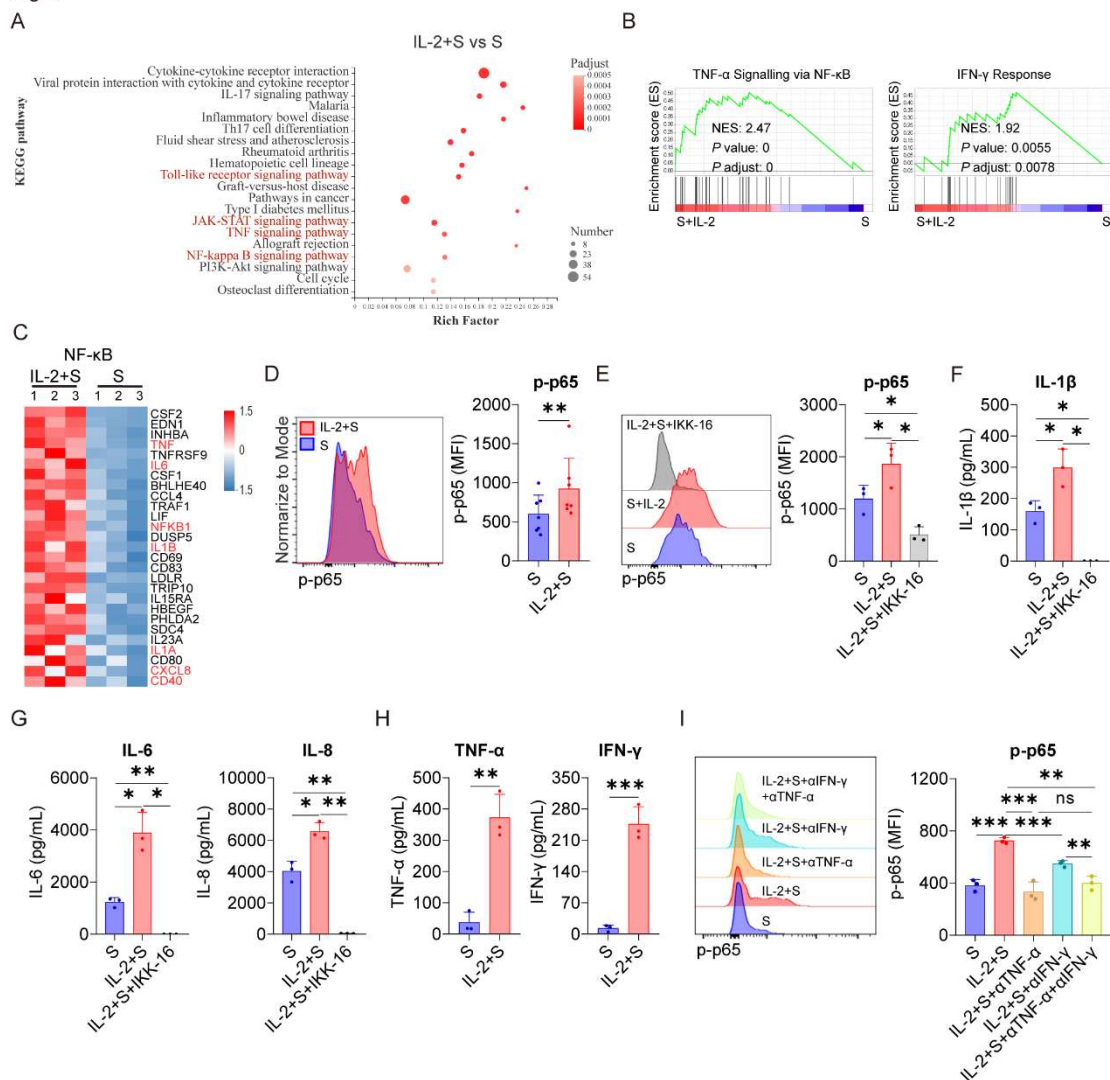
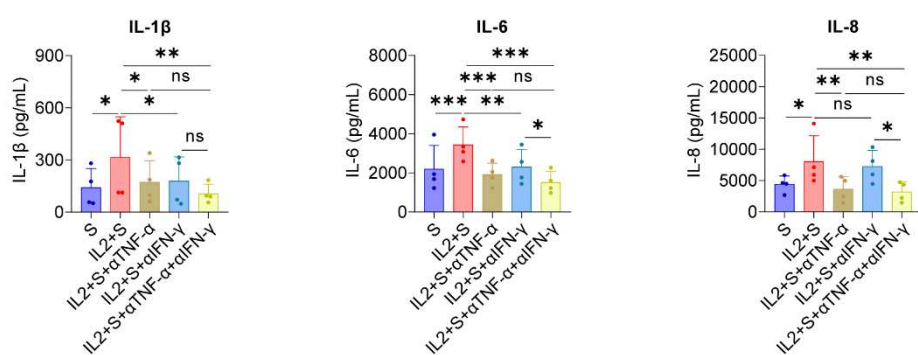
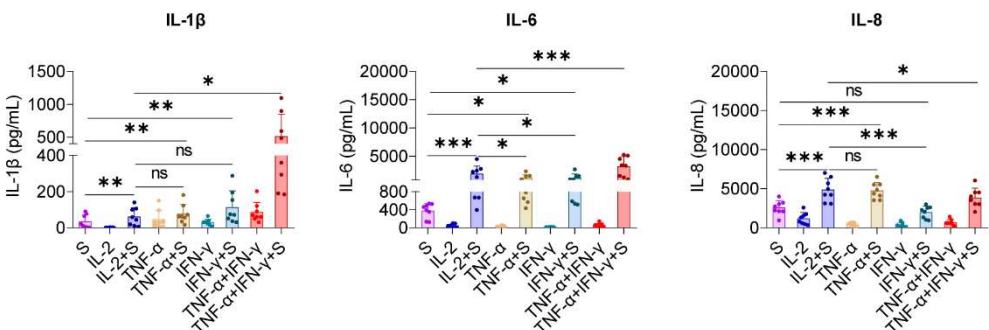


Fig. 4

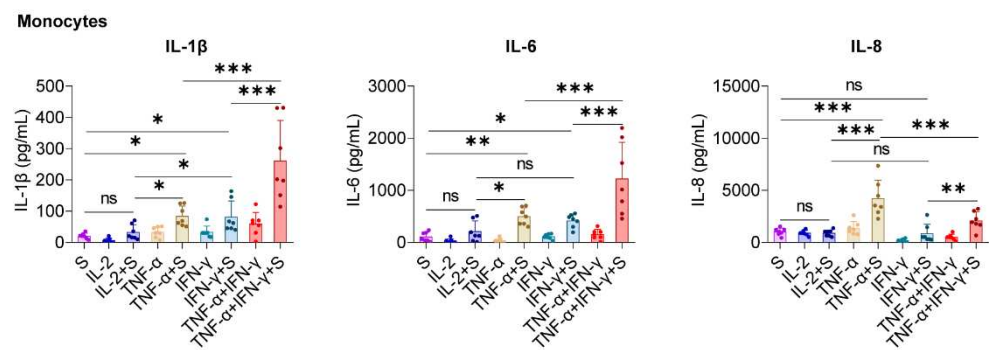
A



B



C



D

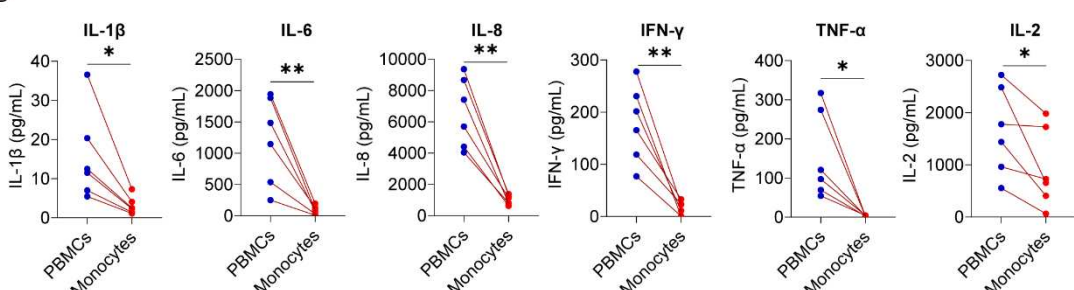
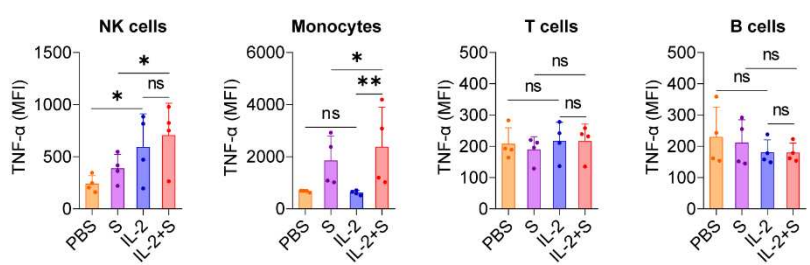
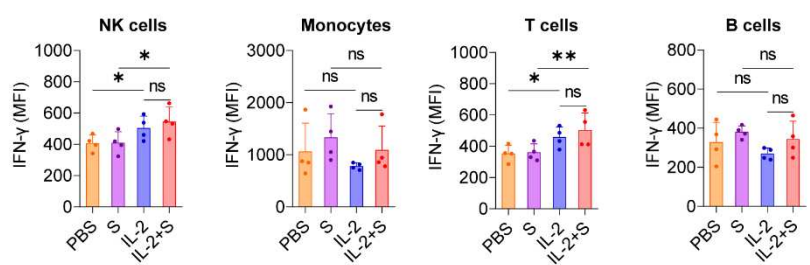


Fig. 5

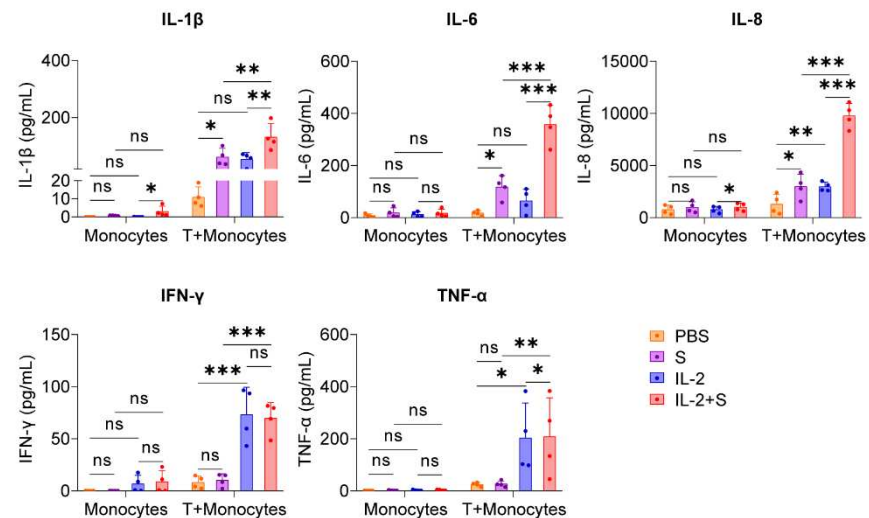
A



B



C



D

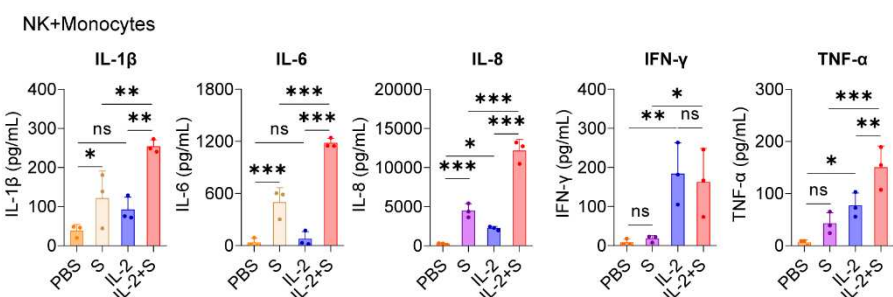


Fig. 6

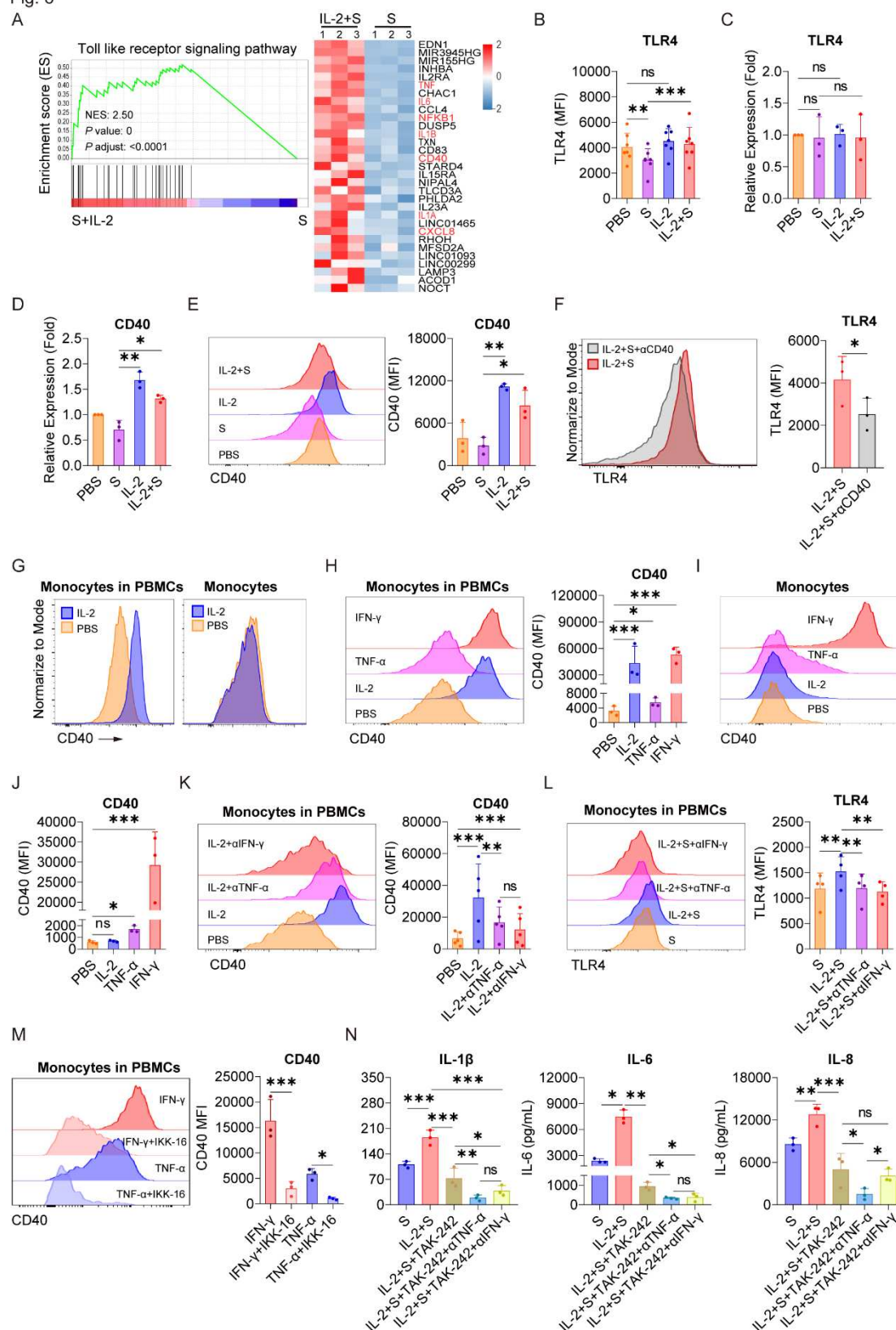
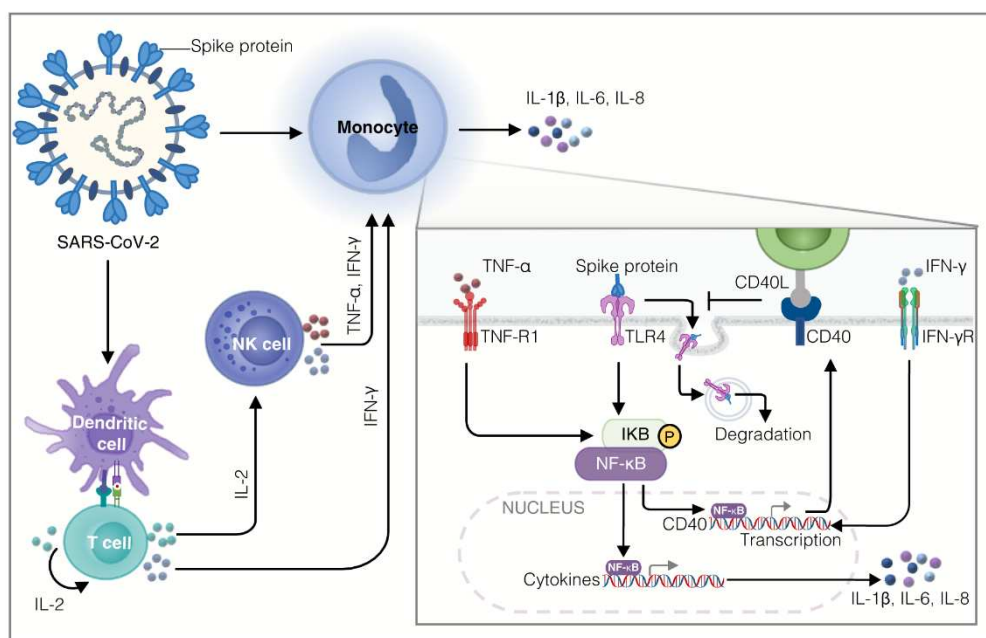


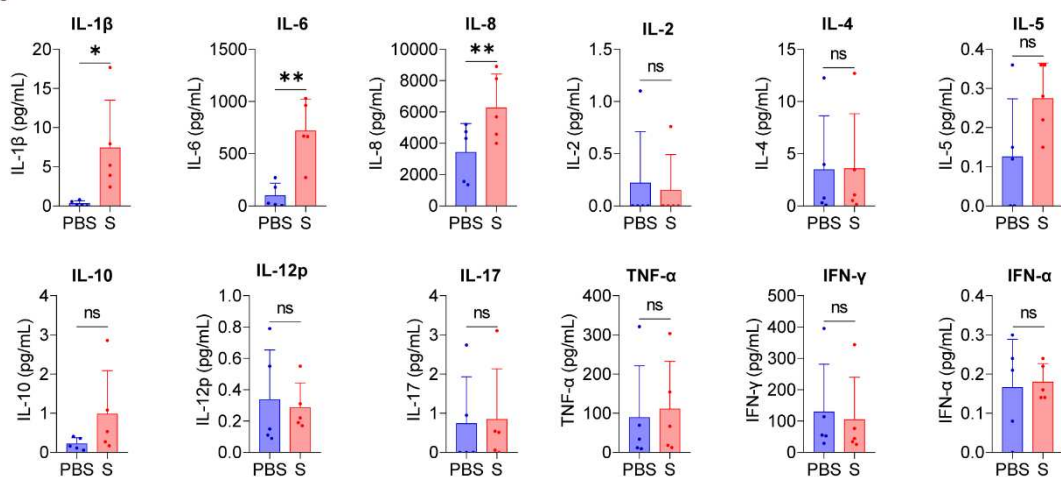
Fig. 7



864

865

Fig. S1



866

Fig. S2

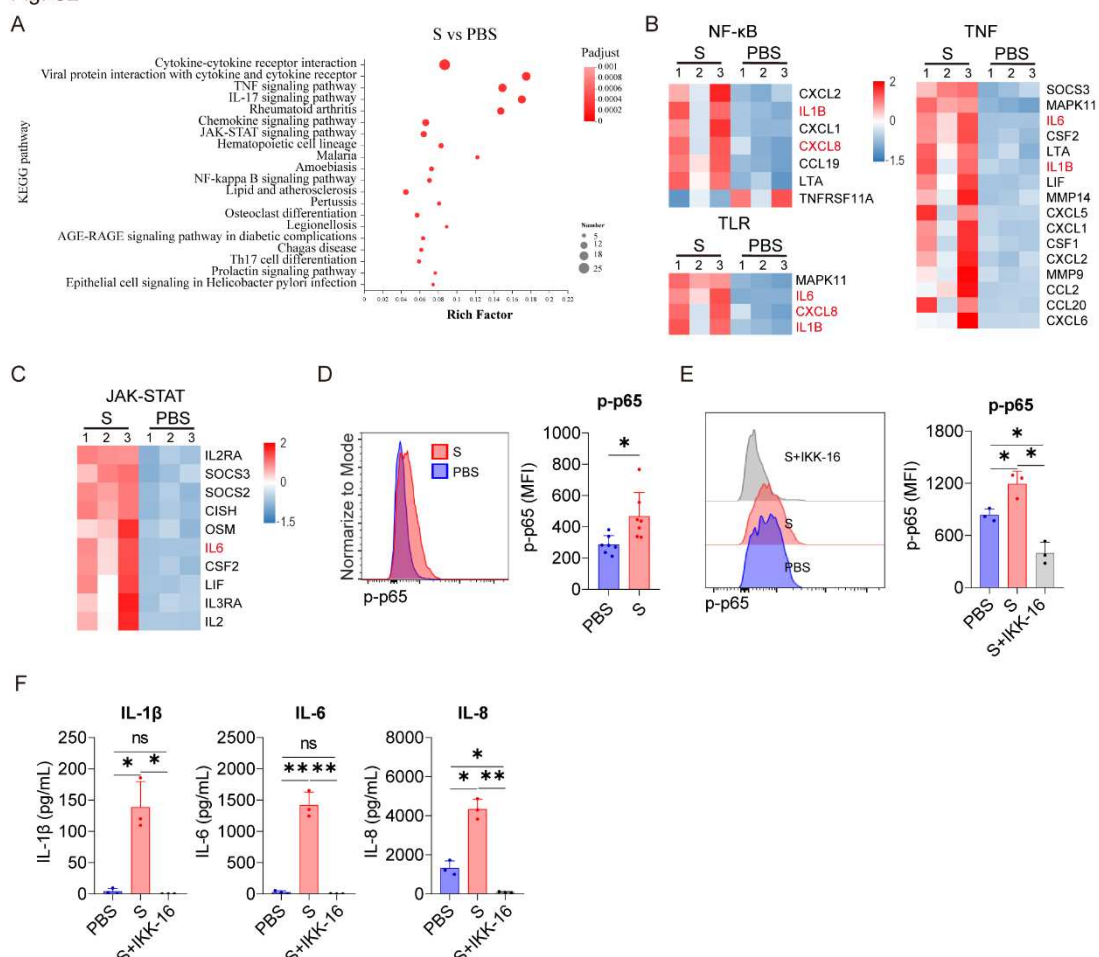


Fig. S3

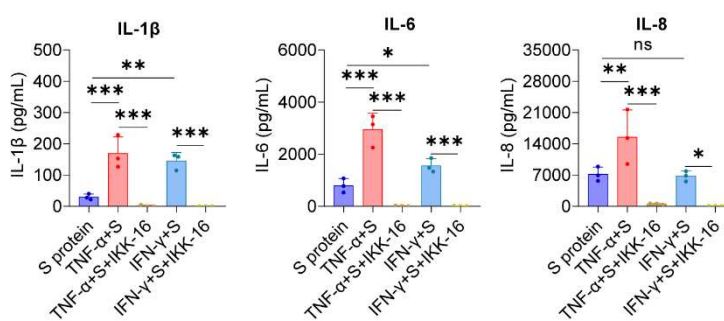
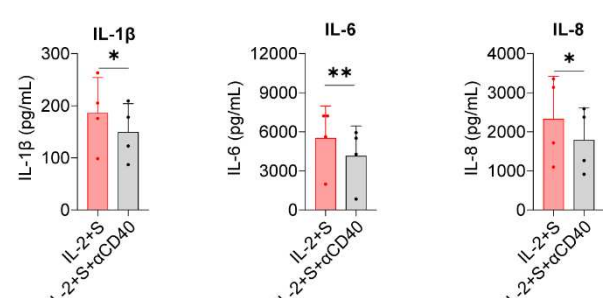


Fig. S4



870 KEY RESOURCES TABLE

REAGENT or RESOURCE	Source of reference	Identifiers	Additional information
<b>Flow cytometry antibodies</b>			
anti-human TNF- $\alpha$	Biolegend	502909	RRID: AB_31526
anti-human IL-6	Biolegend	501120	RRID: AB_2572042
anti-human IFN- $\gamma$	BD Biosciences	554552	RRID: AB_395474
PE Mouse IgG1, $\kappa$ Isotype Ctrl Antibody	Biolegend	400112	RRID: AB_2847829
PE/Cy7 Rat IgG1, $\kappa$ Isotype Ctrl Antibody	Biolegend	400415	RRID: AB_326521
Mouse IgG1, $\kappa$	BD Biosciences	554680	RRID: AB_395506
anti-human CD14	Biolegend	325632	RRID: AB_2563328
anti-human CD40	Biolegend	334307	RRID: AB_1186060
anti-human CD284 (TLR4)	Biolegend	312816	RRID: AB_256248
NF- $\kappa$ B p65 (pS529)	BD Biosciences	558423	RRID: AB_647222
isotype control antibodies	BD Biosciences	559529	RRID: AB_397261
<b>Blocking antibodies</b>			
Ultra-LEAF™ Purified anti-human CD40 Antibody	Biolegend	668103	
Infliximab (TNF- $\alpha$ blocking antibody)	MedChemExpress	HY-P9970	
IFN gamma Monoclonal Antibody (NIB42)	eBioscience	16-7318-81	
<b>Experimental models: cells</b>			
PBMCs	This paper	N/A	
T cells	This paper	N/A	
NK cells	This paper	N/A	
Monocytes	This paper	N/A	
DCs	This paper	N/A	
<b>Software and algorithms</b>			
GraphPad Prim 8	GraphPad Software, LLC	<a href="https://www.graphpad.com">https://www.graphpad.com</a>	
FlowJo V. 10.8	FlowJo, LLC	<a href="https://www.flflowjo.com">https://www.flflowjo.com</a>	
<b>Medium</b>			
RPMI-1640 medium	Gibco	C11875500BT	
CellGenix® GMP DC serum-free medium	CellGenix	20801	
<b>Cytokines</b>			
IL-2	T&L Biological Technology	GMP-TL777	
TNF- $\alpha$	T&L Biological Technology	GMP-TL303	
IFN- $\gamma$	T&L Biological Technology	GMP-TL105	
GM-CSF	T&L Biological Technology	GMP-TL302	
IL-4	T&L Biological	GMP-TL301	

Technology			
Kits			
EasySep™ Human T Cell Isolation Kit	StemCell Technologies	17951	
MACSxpress Whole Blood NK Cell Isolation Kit	Miltenyi Biotec, Bergisch	130-098-185	
EasySep Human Monocyte Isolation Kit	StemCell Technologies	19359	
BD GolgiPlug™	BD Biosciences	555029	
BD Cytofix/Cytoperm™ Plus Fixation/Permeabilization Solution Kit	BD Biosciences	555028	
GeneJET RNA Purification Kit	Thermo Fisher	K0732	
Hifair 1st Strand cDNA Synthesis SuperMix for qPCR	Yeasen	11141ES60	
BD™ Cytometric Bead Array (CBA) Human IL-1 $\beta$ Flex Set	BD Biosciences	558279	RRID: AB_2869135
BD™ Cytometric Bead Array (CBA) Human IL-8 Flex Set	BD Biosciences	558277	RRID: AB_2869133
BD™ Cytometric Bead Array (CBA) Human TNF Flex Set	BD Biosciences	558273	RRID: AB_2869130
BD™ Cytometric Bead Array (CBA) Human IFN- $\gamma$ Flex Set	BD Biosciences	558269	RRID: AB_2869127
BD™ Cytometric Bead Array (CBA) Human IL-6 Flex Set	BD Biosciences	558276	RRID: AB_2869132
BD™ Cytometric Bead Array (CBA) Human IL-4 Flex Set	BD Biosciences	558272	RRID: AB_2869129
BD™ Cytometric Bead Array (CBA) Human IL-2 Flex Set	BD Biosciences	558270	RRID: AB_2869128
BD™ Cytometric Bead Array (CBA) Human IL-10 Flex Set	BD Biosciences	558274	RRID:AB_2869131
Human IL-6 ELISA kit	DAKEWE	1110603	
RealStar Green Fast Mixture	GenStar, Beijing, China	9AC01	
Reagents			
TRIzol™ Reagent	Thermo Fisher	15596026	
BD Cytofix™ Fixation Buffer	BD Biosciences	554655	
BD Phosflow™ Perm Buffer III	BD Biosciences	558050	
SARS-CoV-2-S protein, His Tag, Super stable trimer	ACROBiosystems	SPN-C52H9	
Lymphoprep™	Axis-Shield	1114547	

